Probwind D10: Pre-standard for Probabilistic Design and Background Document

Zhang, Xiaodong; Kelly, Mark; Dimitrov, Nikolay Krasimirov; Nielsen, Jannie Sønderkær; Kalathiparambil Abeendranath, Abhinav; Sørensen, John Dalsgaard

Publication date:
2023

Document Version
Publisher's PDF, also known as Version of record

PROBWIND

DATA-DRIVEN PROBABILISTIC
DESIGN OF WIND TURBINES

D10: PRE-STANDARD FOR PROBABILISTIC DESIGN AND BACKGROUND DOCUMENT

Prepared by:
Xiaodong Zhang, Mark C. Kelly, Nikolay Krasimirov Dimitrov, DTU
Jannie S. Nielsen, Abhinav K. Abeendranath, John D. Sørensen, Aalborg University, AAU
Delivery date: August 2023

This project has received funding from EUDP
Project number 64019-0587.

SUMMARY

This report describes the work done in relation to WP 6 – Recommendations for IEC TC88 Standard / Technical Specification. Based on the results from the previous WPs this WP formulates and prepare recommendations through a pre-standard for a new IEC standard / Technical Specification for probabilistic design.

In T6.1: Background report, the results from WP2 – WP5 are collected in a background document on probabilistic design methods. In T6.2: Pre-standard for probabilistic design of wind turbines, a first draft – a pre-standard - with the main sections and informative annexes in a new standard for probabilistic design is prepared providing input to the MT09 project team. Models and frameworks are developed for low cost design of wind turbines and offshore substructures using probabilistic methods and the validation process through different types of tests and measurements. This report describes the outcome of these two tasks.

CONTENTS

1 INTRODUCTION

Wind energy is becoming more and more important as a main contributor to the production of renewable energy. To sustain this global growth scenario, measures must be taken to meet the requirements brought upon the business by e.g. the competition from other renewable sources of energy (primarily photovoltaics solar). The aim of ProbWind is to improve the competitiveness of wind energy by: a) developing a pre-standard for probabilistic design and b) demonstrating reduction in Levelized Cost of Energy (LCoE) while maintaining the required reliability in the next generation of wind turbine designs.

Design of wind turbines traditionally uses the approach of partial safety factors for a variety of inputs, typically resulting in conservative material use in the wind turbine designs. Instead, ProbWind demonstrates the application of probabilistic methods to utilize available data to design wind turbines to a given reliability level without requiring safety factors, Probabilistic design makes it possible to use the huge amount of data on site conditions, loads, strengths, load effects and degradation collected over several decades by wind turbine manufacturers and operators. The probabilistic design methodology is at level two in the design approaches given in ISO 2394 (2015) where application of partial safety factors is at level one and the much more advanced and complex risk-informed design approach is at level three.

The main standard used in wind turbine design (IEC 61400-1, 2019) opens up for some application of probabilistic design, but still based on the traditional safety factor approach. In ProbWind contributions to the basis for a new international standard / technical specification (TS) on ‘Probabilistic design measures for wind turbines’ is developed. The new technical specification is developed in parallel with the ProbWind project and this report describes some of the main inputs to the TS from this project. Several members of the ProbWind project have contributed to the TS development on key positions including convenorship and coordinators of key chapters making it possible to transfer knowledge and results and coordinate the technical work. The TS is at the end of the ProbWind project at the CD (Commented Draft) stage and is expected to be published in 2024.

The main chapters in the new TS are 1) Introduction, 5) Principal elements (Target Reliability Level and Component Classes, Limit States), 6) Uncertainty representation and modelling (Types of uncertainty, Interpretation of probability and treatment of uncertainty, Probabilistic model, Uncertainties for wind turbines, External condition uncertainty modelling, Load uncertainty modelling, Extreme loads, Fatigue loads, Structural resistance uncertainty modelling, Material properties, Resistance models, Fatigue strength and damage accumulation), 7) Performance modelling, 8) Assessment of reliability (Reliability measures, Computation of failure probability, Reliability-based method, Semi-probabilistic method), 9) Site suitability analysis (Reliability models for site suitability analysis, Site specific uncertainty modelling, Reliability assessment) and annexes on A) Uncertainty quantification, B) Inverse FORM, C) Example Calculations for Reliability Assessment, D) Formulation of Event Driven Design Load Cases, E) Updating of distributions based on evidence, F) Example of the relative approach to site suitability assessment, G) Uncertainty scenarios for site specific wind assessment.

In this report chapter 2 presents a general approach for a pre-standard for probabilistic design of wind turbines. Standardization for probabilistic design / reliability-based structural design has been discussed intensively in the Joint Committee on Structural Safety (JCSS). The main sections proposed for a pre-standard for wind turbine structural design are proposed to follow the proposal in [Madsen & Ditlevsen 1996]. The sub-sections describe the overall models and frameworks needed for low cost design of wind turbines and offshore substructures using probabilistic methods. Finally the content in the CD version of IEC TS 61400-9 is presented.

In chapter 3 background models and information for IEC TS 61400-9 are presented, including Background of the ETM and NTM Turbulence models, Background of the EOG model, Background of Reliability levels, Target reliabilities based on economic optimization for structures – systematic reconstruction, Target reliabilities – no reconstruction after failure, Risk-based assessment of the reliability level for extreme limit states in IEC 61400-1, Target reliability level for seismic sites.

Chapter 4 presents Examples and baseline calculations including Discussion on uncertainty quantification, Bayesian methods for uncertainty quantification, Uncertainty quantification using the Maximum likelihood method, Example on uncertainty propagation, and Baseline model – background for the safety factors.

2 PRE-STANDARD FOR PROBABILISTIC DESIGN OF WIND TURBINES

2.1 GENERAL

This chapter presents a general approach for a pre-standard for probabilistic design of wind turbines. Standardization for probabilistic design / reliability-based structural design has been discussed intensively in the Joint Committee on Structural Safety (JCSS) and a draft content has been included as an Annex in [Madsen & Ditlevsen 1996]. The main sections proposed for a pre-standard for wind turbine structural design are proposed to follow the proposal in [Madsen & Ditlevsen 1996]. The following sub-sections describe the overall models and frameworks needed for low cost design of wind turbines and offshore substructures using probabilistic methods. More detailed content is presented in the following chapters.

The proposal in [Madsen & Ditlevsen 1996] has the following chapters:

- General
- List of symbols
- Concept of adverse state
- Basic variables and uncertainty modelling
- Concept of event margin
- Reliability requirements
- Action modelling
- Structural resistance modelling
- Reliability models
- Reliability calculation methods

This proposal is mainly developed for use in civil / structural engineering. In the following subsections each of these chapters is briefly described and draft content for standard for wind turbines presented. The text from [Madsen & Ditlevsen 1996] are shown in *italic.* … indicates that text are skipped.

2.2 CONCEPT OF ADVERSE STATE

The structural performance of a structural component or system is assumed to be described by a set of adverse states describing when the structure does not satisfy the performance requirements.

Content for general structural systems

Examples of adverse events are:

- *rupture of critical sections of the structure caused by exceeding the ultimate strength possibly reduced by repeated loading, or the ultimate deformation of the material*
- *loss of static equilibrium of the structure*
- *loss of stability,*
- *failure by fatigue load exceeds fatigue resistance*
- *deformations which affect the efficient use or appearance of structural or non-structural elements*
- *excessive vibrations producing discomfort*

Content for wind turbines

Examples of adverse events are:

- Ultimate Limit States (ULS)
    - failure of component or system due to extreme load effects exceeding the ultimate strength
        - during normal operation
        - when wind turbine is in normal operation and a fault occurs
        - when wind turbine is parked
    - loss of stability e.g. buckling
    - loss of static equilibrium / overturning of the wind turbine
- Fatigue Limit State (FLS)
    - failure by fatigue load exceeds fatigue resistance for e.g. welded details in tower or steel substructure, cast steel components, blades. Fatigue failure is generally modelled by the SN-approach and Miners rule; or in special cases by the fatigue crack size exceeds critical crack size (fracture mechanics approach)
- Serviceability Limit State (SLS)
    - failure due to excessive permanent deflection e.g. tilt exceeding an allowable rotation of 0.5°
    - Cracks in reinforced concrete elements due to being subjected to tension stress
- Accidental Limit State (ALS)
    - may be relevant for offshore wind turbines in connection to e.g. ship collision

2.3 BASIC VARIABLES AND UNCERTAINTY MODELLING

Content for general structural systems

Among the parameters of relevance some are presented as being basic variables in the sense that they are assumed to carry the entire input information to the mechanical model. Basic variables are introduced as parameters representing material parameters, external action parameters, and geometric parameters. Basic variables may more generally be functions in time and space. Statistical uncertainty should be taken into account. …

Uncertainties from all essential sources must be evaluated and integrated into the reliability model. Types of uncertainty to be taken into account are physical (intrinsic) uncertainty, statistical uncertainty, and model uncertainty.

If some input variables represent information from prototype testing the joint distributional type of these variables must follow from a mechanical model of the prototype test. …

Content for wind turbines

Basic, stochastic variables shall be formulated for extreme, ultimate limit states and for fatigue limit states. The stochastic variables shall model all relevant physical, model and statistical uncertainties. A Bayesian statistical approach should be applied (See Section 4.2 for details).

The stochastic variables should be standardized by default distribution types and coefficients of variation (COV). Indicative values for illustration of stochastic variables for ultimate limit states (extreme loads) for onshore wind turbine are shown in Table 2.1 based on probabilistic models in [Tarp-Johansen et al. 2002, 2003, 2005, 2006], [Abdallah 2015], [Agarwal 2008], [Toft 2010], [Veldkamp 2006], [de las Heras 2013], [Sørensen & Toft 2010, 2014]. Model uncertainties should be related to a specified model and in addition to the distribution type and COV also the bias should be given. Table 2.2 gives an example of stochastic models relevant to be used together with resistance models in the Eurocodes, see [Vrouwenvelder et al. 2023].

Variable		Distribution	Expected value	COV	
				Normal Operation	Parked / Idling
Q	Physical uncertainty - annual maximum load effect	G/W		0.05-0.15	0.2-0.4[1] 0.3-0.6[2]
X_{Site}	Model uncertainty – site assessment	LN	-	0.1-0.2	0.05-0.15
X_{Aero}	Model uncertainty – aerodynamics	LN	-	0.1-0.15	0.1-0.15
X_{Dyn}	Model uncertainty – aeroelasticity	LN	-	0.05-0.15	0.05-0.15
X_{Mat}	Model uncertainty – material parameters	LN	-	0.05-0.15	0.05-0.15
X_{Wind}	Model uncertainty – wind model	LN	-	0.05-0.15	0.05-0.15
X_{Sim}	Model uncertainty – statistical uncertainty[1]	LN	-	0.05-0.15	0.05-0.15

Table 2.1. Example of stochastic model for ultimate limit states (extreme loads) for onshore wind turbines. G: Gumbel, W: Weibull, LN: LogNormal.

Variable		Distribution	Expected value	COV
R_{Steel}	Yield strength – steel	LN		0.05
X_{Steel}	Model uncertainty – resistance (using Eurocodes	LN	1.15	0.05
$R_{Concrete\ reinforcement}$	Reinforcement strength	LN		0.045
$X_{Concrete\ bending}$	Model uncertainty – bending (using Eurocodes	LN	1.03	0.07
X_{Str}	Model uncertainty – load effect	LN		0.05-0.10

Table 2.2. Example of stochastic models for resistances. LN: LogNormal.

Note – for ULS, a characteristic value for deterministic design can be defined such that the resulting load effect is defined as a load effect with an annual probability of exceedance equal to or less than 0.02, i.e. a load effect whose return period is at least 50 years. This may be important for the probabilistic modelling of especially model uncertainties.

For offshore wind turbines the load effects related to wave loads may be modelled accounting for long-term uncertainties including met-ocean modelling, model an statistical uncertainties;

[1] Extratropical conditions
[2] Tropical / typhoon conditions

and short-term uncertainties related to extreme wave loads dung a storm, a sea state or a wave event including breaking wave effects (non-linear, spilling, breaking, ...). For more information, see e.g. LOADS reports at:
https://www.dropbox.com/sh/7yw4hz7yaq84acq/AAALLLEHH6YqvZBDcSNOHIURa?dl=0 and also https://www.iogp.org/event/2022-offshore-structures-reliability-conference-osrc/ . It is noted that these reports are considering offshore platforms, but some of the new knowledge obtained may be relevant for offshore wind turbines, especially structural components in the upper water column for jacket type substructures.

Examples of stochastic variables for fatigue limit state related to welded steel details are shown in Table 2.3 partly based on information in [Sørensen & Toft 2014], [DNV-RP-C203:2021] and [DNV-RP-C210:2021].

Variable		Distribution	Expected value	Standard deviation
Δ	Model uncertainty – damage accumulation for welded details	LN	1	0.3
X_{SCF}	Model uncertainty – stress analysis	LN	-	0.05-0.1
X_W	Model uncertainty – fatigue load	LN	-	0.03-0.2
m_1	Upper slope – bilinear SN-curve	D	3	
$\log K_1$	Bilinear SN-curve	N		0.2
m_2	Lower slope – bilinear SN-curve	D	5	
$\log K_2$	Bilinear SN-curve	N		0.2

Table 2.3. Example of stochastic model for fatigue of welded steel details. D: Deterministic, N: Normal, LN: LogNormal. log K_1 and log K_2 are assumed to be fully correlated.

2.4 CONCEPT OF EVENT MARGIN

Content for general structural systems

An event margin corresponding to a specified event is defined as a function of the basic variables with the property that it takes a negative value if and only if the event occurs.

...

Content for wind turbines

Examples of event margins relevant for wind turbines are

- No-detection of (surface) cracks in connection with inspections for cracks in welded details in tower or substructure of offshore wind turbines, cast steel components and blades, the event margins are modelled equivale t to limit state margins by introducing Probability Of Detections (POD) corves to model the reliability of the inspections.
- Detection of a crack / damage with a measured crack / damage size.
- No failure of wind turbine components or system at a specified point in time.

2.5 RELIABILITY REQUIREMENTS

Content for general structural systems

Decision theoretical principles can be applied in order to obtain optimal reliability levels. It is required, however, that the intangible part of the cost of failure is chosen such that it is comparable in value to the population of failure costs associated with present code based *engineering practice when declaring this practice to be optimal. ... Optimal reliability levels depend on the reference period. ... Required minimal reliability levels make sense only together with a specification of a reference period. The reference period should generally equal the anticipated lifetime of the structure (e.g. 100 years) ... For the reliability measure defined herein the required levels are obtained by calibration to structural dimensions following from present code based engineering practice ...*

Content for wind turbines

Reliabilty requirements can be specified by a target reliability level associated with a target probability of failure and by a minimum reliability associated with a maximum probability of failure. The failure probabilities are to be associated to

- Consequence of failure, which for wind turbines are economic expenses and in rare cases human fatalities / injuries. Consequences of failure are classified as low, medium and high.
- Relative cost of safety measure associated with the cost to obtain a certain reliability level. It is classified as small, medium and large.
- A reference period which can be e.g. 1 year or the design lifetime of the wind turbine f.x. 25 years.
- Components or systems. Different components may be designed to different reliability levels.
- Failure modes being ductile or brittle which can be important for the consequences and of the costs of mitigation of a failure.

As an illustration based on [IEC 61400-1:2019] and [DNV-ST-0126:2021] a target and a minimum reliability level may be defined by an annual target probability of failure equal to 10^{-4} and a minimum reliability of failures by a maximum annual probability of failure equal to $5\ 10^{-4}$. These failure probabilities are assuming ductile failure modes, and implicitly low to medium consequence of failure and medium to large cost of safety measure. Further, these reliability levels are associated with components assuming that mainly one or a few correlated failure modes are dominating, and components are classified in three component classes.

The reliability levels may be based calibration to historical reliability levels obtained using existing partial safety factors and the standardized stochastic models or by a risk-based cost optimization where the total expected cost-benefits in the lifetime is optimized.

It is noted that the reliability requirements can be used for deterministic (semi-probabilistic) or reliability-based 1) design of new wind turbines, 2) life extension of existing wind turbines and 3) for planning of inspections and monitoring.

2.6 ACTION MODELLING

Content for general structural systems

The action models set up for structural reliability analysis must be given sufficiently detailed structure to allow reasonable treatment of action effects caused by the random variation of the actions across the structure and in time. Furthermore, the models should allow the study of combined action effects due to several simultaneous actions...

For most reliability investigations it is not essential that the action models reproduce the individual action effect histories in their details. The approximate reproduction of the basic probabilistic properties of the action effect histories is often sufficient. Standardized *distributions and process types to be used in action models for specific reliability investigations can be given in an action code to be used in parallel with this code on reliability methods. In such cases the action load model standardizations given in this code are secondary to the standardizations of the action code.*

Content for wind turbines

The actions relevant for wind turbines are first of all the wind actions, but also actions du e to gravity, earthquakes, waves, current and ice are important. Design standards such as [IEC 61400-1:2019] and [IEC 61400-3-1:2019] includes probabilistic modelling of some of the actions and deterministic models for other actions. For probabilistic modelling of the actions see section 2.3.

Probabilistic modelling of action effects has to take into account the non-linear behavior mainly due to the control system of the wind turbine. Design standards such as [IEC 61400-1:2019] and [IEC 61400-3-1:2019] includes probabilistic modelling of some of the action effects. The action effects should be modelled for the Design Load cases (DLCs) in as [IEC 61400-1:2019] and [IEC 61400-3-1:2019] including 1) normal operation, 2) normal operation with fault, 3) start up and shut down stages, and 4) parked / idling stages. For probabilistic modelling of the actions some aspects are included in section 2.3.

2.7 STRUCTURAL RESISTANCE MODELLING

Content for general structural systems

The reliability requirements of this code are for specific failure modes of structural elements such as bars, beams, columns, plates, walls etc. The reliability analysis of larger structural subsystems or the entire structural system must be made in order to investigate whether there are significant system effects on the reliability, and in particular whether such effects are to the side of serious decrease of the reliability.

This code allows the use of decision analytical principles to obtain reasonable system reliability levels provided an assessment of the intangible costs of failure has been made as required…

Standardized distributions of material properties to be used in structural resistance models can be given in material oriented codes to be used in parallel with this code on reliability methods. Standardized distributions given in such material codes are superior to the standardizations given in this code. It is required that a standardized distribution of a material property assigns zero probability to any set in which no value is possible due to the physical definition of the considered material property.

The requirement of zero probability on physically impossible sets is formulated for guidance of material code writers. It ensures against having for example negative strengths helping the reliability. However, this requirement does not prevent that calculational easier distributions that are not obeying the requirement be used as approximations provided it can be justified that the inconsistency with the physical possibilities contributes insignificantly to the calculated reliability.

Reliability analyses should always be made for each of the structural elements but also to a certain extend for the entire structural system. The structural elements can be defined as smaller or larger subsystems of the entire structural system. …

Content for wind turbines

Modelling of structural resistance of wind turbine structures are generally done by using recognized standards, e.g. the structural Eurocodes EN1992, EN1993 and EN1997 and therefore follows the same principles as for general structural systems. This includes use of standardized stochastic models for physical and model uncertainties to be specified in the probabilistic design code and linked to the specific resistance models used.

2.8 RELIABILITY MODELS

Content for general structural systems

… A standard reliability measure may be chosen to be the generalized reliability index. It is defined as $\beta = -\Phi^{-1}(P_f)$ where Φ is the standardized Normal distribution function. … The probability P_f is calculated on the basis of the standardized joint distribution type of the basic variables and the standardized distributional formalism of dealing with both model uncertainty and statistical uncertainty. The standardized distribution type related to the basic variables of the action models are defined in the action code while the standardized distribution types related to the basic variables of the resistance models are defined in the specific material related codes. If no specific distribution type is given as standard in the action and material codes this code for the purpose of reliability evaluations standardizes the clipped (or, alternatively, the zero-truncated) normal distribution type for basic load pulse amplitudes. Furthermore, the logarithmic normal distribution type is standardized for the basic strength variables. Deviations from specific geometric measures of physical dimensions as length are standardized to have normal distributions if they act at the adverse state in the same way as load variables (increase of value implies decrease of reliability) and to have logarithmic normal distribution if they contribute to the adverse state in the same way as resistance variables (decrease of value implies decrease of reliability). …

In special situations other than the code standardized distribution types can be relevant for the reliability evaluation. Such code deviating assumptions must be well documented on the basis of a plausible model that by its elements generates the claimed probability distribution type. Asymptotic distributions generated from the model are allowed to be applied only if it can be shown that they by application on a suitable representative example structure lead to approximately the same generalized reliability indices as obtained by application of the exact distribution generated by the model.

Experimental verification without any other type of verification of a distributional assumption that deviates strongly from the standard is only sufficient if very large representative samples of data are available. Distributional assumptions that deviate from those of the code must in any case be tested on a suitable representative example structure. By calibration against results obtained on the basis of the standardizations of the code it must be guaranteed that the real (the absolute) safety level is not changed significantly relative to the requirements of the code. The reliability model of this code is a formalistic set of rules that allows engineering decision making on the basis of a mathematically rational processing of available well documented information.

… Alternatively, if the worst case philosophy is not followed the decision maker is given a set of conditional probability statements which honestly can be claimed to predict the relative frequency of occurrence of the adverse event given the truth of the conditioning statements. In a structural reliability context the conditioning statement is in general a conjunction of many conditioning statements of widely different nature. In order that the decision maker can utilize the given probabilistic information he or she must weigh the different conditioning statements against each other. This means that he or she is forced into the problem of combining the conditional probabilities according to the rule of total probability using weighting probabilities that have no direct relative frequency interpretation. These probabilities are called Bayesian probabilities (or subjective probabilities). The mental process of judgment obviously calls for aiding standardizations of distribution types implying that only the values of some few parameters have to be assessed by professional judgment. Design by maximization of utility

(minimization of total cost) can be made within the framework of this code. However, the cost consequence of some adverse event like loss of human life must be calculated on the basis of the postulate that current design practice as it is approved by the authorities is optimal.
...

Content for wind turbines
The same principles apply for wind turbine structural systems as for general structural systems.

2.9 RELIABILITY CALCULATION METHODS

2.9.1 STRUCTURAL RELIABILITY METHODS

Content for general structural systems
The numerical value of the reliability measure is obtained by a reliability calculation method. Due to the computational complexity a method giving an approximation to the exact result is generally applied.
Two fundamental accuracy requirements are:

- *Overestimation of the reliability due to use of an approximative calculation method be within limits generally accepted for the specific type of structure.*
- *The overestimation of the generalized reliability index must not exceed 5%.*

The accuracy of the reliability calculation method is linked to the sensitivity with respect to structural dimensions and material properties in the resulting design. General design practice has inherent rules of acceptable errors since dimensions and material properties are often only available in discrete classes. An error larger that 5% is rarely accepted.
When the modeling of the basic random variables is in terms of a random vector the first order reliability method (FORM) in general results in a sufficiently accurate approximation to the reliability measure…
If no prior experience with the specific type of adverse state is available, the FORM result should be checked. This can be done locally around the locally most central points by an asymptotic second-order reliability method (SORM), where the adverse state surface is approximated by a second-order surface at the locally most central points, or by an importance sampling around the locally most central points. Globally it should be checked that the most central point has been identified. This can be done by a Monte Carlo simulation, e.g., using directional sampling. Besides computing the reliability measure it is recommended to check the sensitivity of this reliability measure to all input parameters, i.e., the deterministic basic variables and distribution parameters for the random basic variables. The asymptotic results for the sensitivity of the generalized reliability index are in general sufficiently accurate for this task.

Content for wind turbines
The same principles apply for wind turbine structural systems as for general structural systems, i.e. the probability of failure can be estimated by FORM/SORM methods or by simulation techniques where crude Monte Carlo simulation becomes more and more relevant with the increasing power of computers.

Alternatively, as being investigated to be introduced in design standards for offshore structures and already applied in design standards for seismic design (e.g. Eurocode prEN 1998:2023) the fragility curve approach can be computationally efficient. In the following subsection a short description of this approach is presented with comments on potential application for wind turbines, especially offshore wind turbines.it is noted that this approach is not directly mentioned in [Madsen & Ditlevsen, 1996].

2.9.2 FRAGILITY CURVES AS A SIMPLIFIED PROBABILISTIC DESIGN METHOD

Fragility curves are

- Developed and used for seismic loads, e.g. in Eurocodes prEN1998-1:2023
- Considered to be implemented in ISO 19900 standards for offshore platforms for oil & gas as a 'simple' way to estimate the reliability
- Considered in a number of papers to be used for wind turbines

Figure 2.1 illustrates the Hazard and fragility curves modelling the probability of exceedance of a chosen load effect equal to an Intensity Measure, IM, and a Fragility curve modelling the probability of failure given IM. The Hazard curve mainly models the load effect and the Fragility curve the resistance, but part of the uncertainty related to load effects may be included in the Fragility curve.

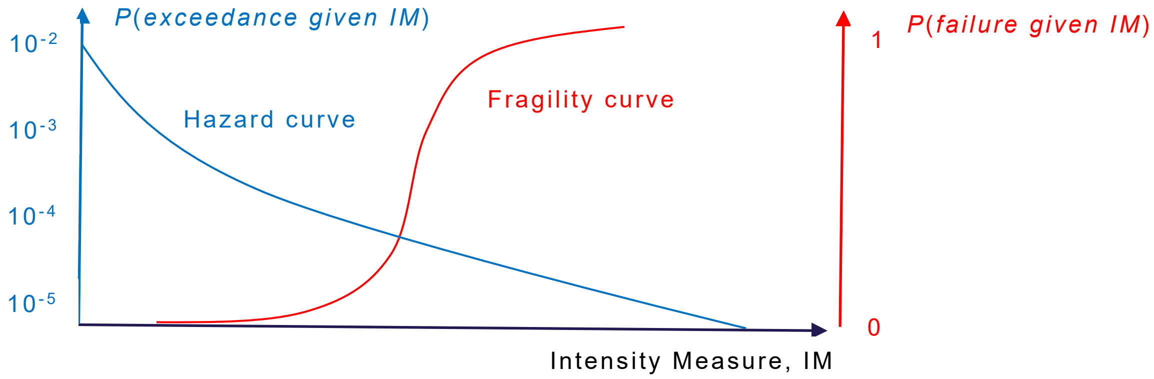

Figure 2.1. Fragility and Hazard curves as functions of the Intensity Measure, IM.

The probability of failure is estimated by:

$$P_f = \int F_R(IM)\ f_S(IM)\ d\,IM \qquad (2.1)$$

or

$$P_f = \int f_R(IM)\ \left(1 - F_S(IM)\right)\ d\,IM \qquad (2.2)$$

where

IM Intensity Measure

$F_R(IM)$ Fragility curve: probability of failure given IM = probability distribution function of resistance given IM.

$1 - F_S(IM)$ Hazard function, $H(IM)$: probability of exceedance function for load effect given IM.

Examples of Intensity measures IM:

- Earthquakes:
  - Peak Ground Acceleration, PGA
- Offshore structures:

  - Spectral base shear
- Onshore wind turbines:
  - Mean wind speed (Quilligan et al. 2013)
- Offshore wind turbine support structures:
  - Mean return period (RPM) of wave (significant wave height) and wind (1h mean wind speed), (Wilkie et al. 2020)
  - Mean wind speed and significant wave height, (Hallowell et al. 2018), (Mardfekri & Gardoni 2013)
- Typhoons: wind speed and significant wave height (Sheng & Hong 2021)

Equation (2.1) can be extended to include e.g. maximum load effects (stresses) from combined bending and axial forces as a temporary load effect, *EDP*:

$$P_f = \int F_R(EDP)\ f_{EDP}(EDP|IM)\, f_S(IM)\ d\,EDP\ \ d\,IM \qquad (2.3)$$

where

$f_{EDP}(EDP|IM)$ is the probability density function of *EDP* given *IM* and is typically modelled as Lognormal with COV related to the short-term variability in the turbulent wind and irregular wave processes

$F_R(EDP)$ is the fragility curve as a function of *EDP*

Fragility and hazard curves are widely used in seismic engineering where large simplifications are introduced. The following simplifications are introduced:

The fragility curve is assumed Lognormal distributed with distribution function:

$$F_R(IM) = \Phi\left(\frac{\ln IM - \theta}{\beta}\right) \qquad (2.4)$$

where the intensity measure, *IM* is related to the spectral acceleration S_e and

$\theta = \ln \mu$ with μ being the median

β is the logarithmic standard deviation

β is approximately equal to the COV of the fragility curve (resistance function)

The hazard function is for part of the interval of the *IM* be assumed linear in logarithmic scale:

$$1 - F_S(IM) = H(IM) = C\ IM^m \qquad (2.5)$$

where

C is a parameter

m is the slope of the hazard function in logarithmic scale

By these approximations the probability of failure can be obtained from

$$P_f = \int f_R(IM)\ \left(1 - F_S(IM)\right)\ d\,IM \qquad = \int f_R(x)\, H(x)\, d\,x = \exp\left(\frac{1}{2}m^2\beta^2\right)\ \ C\,\mu^k \qquad (2.6)$$

Introducing a value $IM = X_{PF}$ of the Hazard curve with return period $T_{PF} = 1/(C\, {X_{PF}}^{-m})$ then

$$P_f = \frac{1}{T_{PF}}\left(\frac{\mu}{X_{PF}}\right)^m \exp\left(\frac{1}{2}m^2\beta^2\right) \qquad (2.7)$$

In prEN1998-1:2023 $m = -k,\ T_{PF} = T_{ref},\ X_{PF} = S_{e,ref}$ and $\mu = S_{e,LS}$.

It is noted that given a target annual probability of failure P_f

- a characteristic value of the hazard curve (load) can be obtained, e.g. $X_{PF}\, with$ a return period of 1 / $P_f = 1/(C\, X_{PF}{}^{-m})$ and
- a characteristic value of the strength, e.g. the median μ, then
- a 'partial safety factor' can be obtained from $\gamma_R = \exp\left(-\frac{1}{2} m\, \beta^2\right)$

The advance of the above fragility curve approach is that 'light' probabilistic design can easily be performed if it can be assumed that the hazard curve is approximately linear in logarithmic scale with slope m and the fragility curve is Lognormal distributed with COV equal to β which may be standardized for certain types of structures (and failure modes). For offshore platforms m = 10 and β = 0.3 could be representative. For offshore wind turbines similar representative values could be determined. It is noted that multiple failure modes may be difficult include.

Given a target P_f, X_{PF}, m and β the required median resistance of the fragility curve can easily be obtained.

2.10 IMPLEMENTATION IN IEC TS 61400-9

In 2020 the following objectives and background was approved by IEC as the basis for developing a new Technical Specification og 'Probabilistic design measures for wind turbines (from IEC 88/761/NP: NEW WORK ITEM PROPOSAL (NP)):

Develop a new Technical Specification (TS) in the 61400 series with the scope to specify essential requirements to the use of probabilistic design measures in order to ensure the structural and mechanical integrity of wind turbines.

The TS shall be based on the general approach in ISO 2394:2015: General principles for reliability of structures, which also forms the basis for IEC 61400-1 Wind Turbines - Design requirements. In 61400-1 the design verification approach is based on deterministic design using safety factors. However, edition 4 opens for introduction of probabilistic design in an informative annex specifying requirements to the calibration of structural material safety factors and structural design assisted by testing.

The new TS shall supplement 61400-1 by providing appropriate methodologies and requirements for full probabilistic design taking into account specific uncertainties on not only material properties but also on environmental conditions, design models and the degree of validation.

Wind turbines are industrial products using specific materials which are documented by extensive material tests and tests of components and the full structure. Furthermore, wind turbines are installed under various complex conditions, which have been estimated or measured with uncertainties that varies from project to project.

A safe design has so far been ensured using a deterministic design approach using safety factors and wind classes for the external condition, followed by a verification of site suitability. The target design annual probability of failure is in the order 0,5-1 x 10-4, but the approach does not take into account the information from specific tests, site specific measurements and analysis of external conditions, nor will the approach ensure a uniform or consistent reliability across structural and mechanical components.

In general the approach is expected to be conservative, but probabilistic design measures offers considerable cost savings by eliminating unnecessary conservatism, if more precise information than assumed on conditions, loads and resistance uncertainties is available.

Safe wind turbine design are based on a combination of comprehensive computational models for loads and response, data from tests of components and materials, measurements and predictions of climatic conditions and full-scale tests, where performance or loads are measured and used for the validation of the design methods. Hence the information available for the design is subject to physical, model, statistical and measurement uncertainties. These uncertainties can be assessed and combined in probabilistic design, e.g. by use of Bayesian statistical methods.

The TS shall provide the basis for probabilistic design and uncertainty representation, including target reliability levels and safety formats, appropriate probabilistic models for load effects in structural and mechanical components, based on stochastic modelling of the external conditions including the wind and load response, probabilistic design methodology for structural and mechanical components, based on stochastic models for failure modes related to structural and mechanical components incl. effect of failure of electrical components as well as resistance of structural components, blades, foundations, mechanical components.

Furthermore, the TS shall provide requirements to tests and measurements and principles for statistical evaluation of test data. Furthermore, the TS shall provide requirements to tests and measurements and principles for statistical evaluation of tests data, based on the principles as in the annex in IEC 61400-1 ed.4 for materials. Additionally the TS shall provide reliability-based requirements to account for inspections in the design securing the required reliability level and optimizing the life-cycle based LCOE.

As the first step in developing the new TS a CD (Commented Draft) version was developed and submitted for comments. The content of the CD version consists of 9 chapters and 7 annexes and is as follows:

It is seen that the content to a large degree follows the framework for the pre-standard presented in sections 2.1-2.9. In the next chapters selected background developed during the ProbWind project for the content of some of the chapters in the TS is presented.

3 BACKGROUND OF IEC61400-9 MODELS

3.1 BACKGROUND OF THE ETM AND NTM TURBULENCE MODELS

The IEC 61400-1 standard series prescribe a number of design load cases (DLCs) where the design integrity of the turbine is verified against a range of environmental conditions and operating scenarios. While the specifications of environmental conditions in the 61400-1 DLCs have mostly deterministic formulations, the values for a number of DLCs are based on probabilistic considerations in terms of statistical distributions and event return periods. This section highlights the underlying probabilistic models serving as a basis for the NTM (Normal Turbulence Model) and ETM (Extreme Turbulence Model) definitions in IEC61400-1. These definitions are also adopted in IEC61400-9.

The IEC models define the 10-minute average wind speed, u, and turbulence (wind speed standard deviation, σ_u) as jointly distributed. The wind speed u is considered as an independent random variable following a Weibull distribution. In the case of using reference wind classes (I-III), the distribution is specified even more strictly as a Rayleigh distribution, which is a specific case of the Weibull distribution with shape parameter k = 2, with the mean wind speed the only remaining distribution parameter.
The turbulence is defined as conditionally dependent on the mean wind speed. In ed.3 of the 61400-1 standard, the turbulence follows a lognormal distribution, while in ed.4 it follows a Weibull distribution. In both cases, the turbulence distribution parameters are linearly dependent on the mean wind speed. The original calibration of the conditional dependence introduced in ed.3 of IEC61400-1 is primarily based on the measurements presented in [Stork et al.1998]. Later studies and data analyses show that the prescribed form of the dependence is representative for many sites, however the proportionality constants and especially the magnitude of the standard deviation of the turbulence, σ_{σ_u}, can vary significantly and the reference turbulence classes are not completely representative of the range of turbulence variation [Dimitrov et al. 2017].

In order to simplify the calculations and provide the possibility for doing deterministic design procedures, the joint wind-turbulence distribution is used to prescribe representative wind conditions for fatigue and ultimate limit state calculations (the "Normal Turbulence Model", NTM). These models for wind conditions only retain the 10-minute average wind speed as a random variable, while the turbulence is described as a deterministic function of the wind speed. This deterministic function is equivalent to the 90th percentile of the full conditional distribution of turbulence. The 90th percentile is chosen as representative for fatigue load analysis. Typically a wind turbine blade (or other composite component) load assessment procedure using the 90th percentile results in approximately the same lifetime fatigue load estimates as an assessment based on sampling the full turbulence distribution.

The same joint wind speed – turbulence distribution model is behind the definitions for extreme turbulence events prescribed as the Extreme Turbulence Model (ETM). The ETM model prescribes combinations of wind speed and turbulence that have an estimated recurrence period of 50 years – the so-called environmental contours (Figure 3.1). The ETM model is the same in both ed.3 and ed.4 of the 61400-1 standard, and it is based on the lognormal conditional turbulence distribution defined in ed. 3:

$$E[\sigma_u] = I_{ref}(0.75 \cdot V_{hub} + b), \qquad b = 5.6m/s$$
$$Var[\sigma_u] = 1.4 I_{ref} \qquad (3.1)$$

Computing the magnitude of the extreme events and drawing the contours is based on the iFORM (inverse First-Order Reliability Method) approach [Winterstein et al. 1994]. As a further simplification, the actual ETM model defined in IEC61400-1, ed.3 draws straight lines tangential to the actual contours (Figure 3.1).

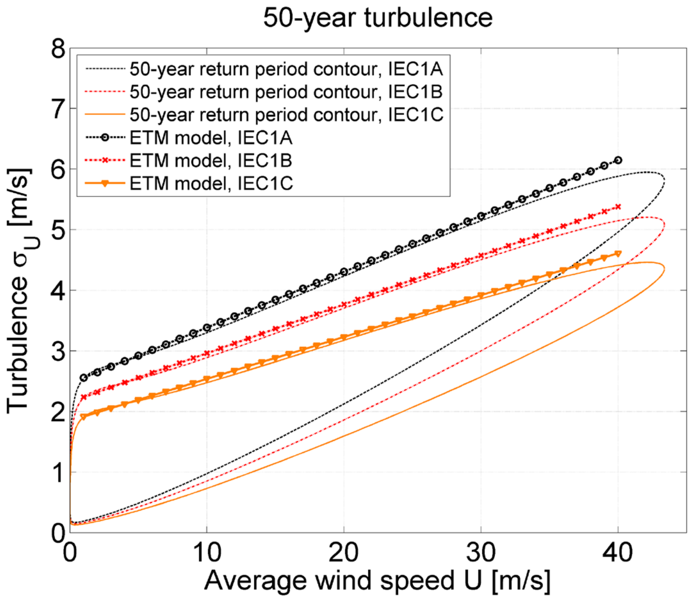

Figure 3.1 Environmental contours example showing the ETM (Extreme Turbulence Model)

The use of the iFORM approach for drawing environmental contours may lead to certain misconceptions. When applying the iFORM method, the return period (and the related exceedance probability) implied by the contour correspond to the total probability of having observations beyond a straight line tangential to a single point on the contour (red area on Figure 3.2). This is appropriate for situations where only the exceedance beyond a single point or a narrow region (e.g. a single extreme combination of wind speed and turbulence) are of interest. In case that a broad range of combinations (i.e., a long portion of a contour) are of interest, the iFORM computations need to be modified to account for the probability of occurrence for the entire space outside the contour (the combined blue and red shaded areas on Figure 3.2), or for an explicitly defined sector [Dimitrov 2020]. This is possible by replacing the Gaussian distribution in the formula for computing the contour radius β with a Chi-squared distribution:

$$\beta = \sqrt{\chi_M^{inv}(1 - p_r)} \qquad (3.2)$$

where p_r is the exceedance probability, and χ_M^{inv} denotes the inverse chi-squared distribution with M degrees of freedom.

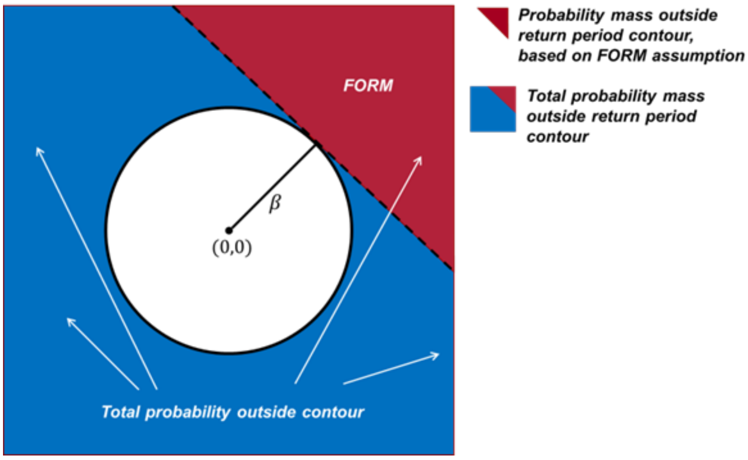

Figure 3.2 Difference between probabilities assumed by the iFORM and the total probability outside a contour. Picture taken from [Dimitrov 2020].

3.2 BACKGROUND OF THE EOG MODEL

3.2.1 BACKGROUND FOR THE DETERMINISTIC WIND FIELD EVENT EOG

In IEC61400-1 ed. 4, DLC2.3 can be verified using either the deterministic wind field event EOG or using stochastic simulations with NTM. The current formulation of the EOG load was introduced in IEC61400-1 ed.3, and the magnitude was motivated in an unpublished background document [Thesbjerg 2007]. In the following, the background is repeated, in order to put it into the public domain, as knowing the background of the deterministic loads is essential for the development of probabilistic models. In DLC2.3, the EOG wind profile is used together with the abnormal safety factor, as the joint occurrence of an electrical fault (loss of grid correction) with an extreme gust is uncommon. The EOG magnitude was developed on the basis of DLC 3.2 and 4.2, where a startup or shutdown happens at the same time as the gust. The gust is found to give a joint return period of 50 years. The size of the gust is derived based on the Kaimal spectrum.

Since the turbulence is Gaussian, the gust magnitude is also Gaussian and is modelled by the variable Y_2. The gust magnitude is the rise in wind speed in the duration of the relevant rise time of the gust. For the Mexican hat shaped gust with a duration of 10.5 s, the rise time is $T_R = 0.266 \cdot 10.5\,\mathrm{s} = 2.79\,\mathrm{s}$. The variable Y_2 has a mean equal to zero and the standard deviation:

$$\sigma_{y2} = \sigma_1 \sqrt{2(1-\rho(T_R))} \tag{3.3}$$

where $\rho(T_R)$ is the correlation function evaluated at T_R, and σ_1 is the 90% quantile of the turbulence standard deviation given by:

$$\sigma_1 = I_{ref}\left(0.75\, V_{hub} + 5.6\frac{m}{s}\right) \tag{3.4}$$

The correlation length for the turbulence process is:

$$\rho(T) = \int_0^{50Hz} cos(\omega\, T)\, S_1(\omega)\, d\omega \tag{3.5}$$

where the normalized Kaimal power spectrum for the frequency ω is given by:

$$S_1(\omega) = \frac{\frac{4\,L_1}{V_{hub}}}{2\pi \cdot \left(1 + 6 \cdot \frac{\omega}{2\pi} \cdot \frac{L_1}{V_{hub}}\right)^{5/3}} \quad (3.6)$$

where V_{hub} is the 10 minute mean wind speed, and L_1 is the integral length scale given by:

$$L_1 = 8.1\,\Lambda_1 \quad (3.7)$$

where the longitudinal turbulence scale parameter is $\Lambda_1 = 42\,\text{m}$ for hub heights larger than 60m.

The distribution function for the gust size given an event (e.g. startup/stop) is:

$$F_{Y_2}(y_2|E) = \Phi\left(\frac{y_2}{\sigma_{y2}}\right) \quad (3.8)$$

Assuming a Poisson process for the occurrence of events with rate f_T, the quantile corresponding to a return period of T_p is given by $1 - P_N$:

$$P_N = \frac{1}{f_T \cdot T_p} \quad (3.9)$$

DLC 3.2 and 4.2 (Startup / Normal shutdown)

For a return period $T_p = 50$ years, the extreme gusts were in [Thesbjerg 2007] evaluated for DLC3.2 and 4.2 (startup/stop) for $I_{ref} = 0.16$ and compared with the extreme gust in IEC61400-1 $V_{gust} = 3.3\,\sigma_1$ for three wind speeds. The results are given in Table 3.1. Figure 3.3 shows the probability of exceedance for gust magnitudes for each wind speed, and the quantiles corresponding to a combined 50 year event with startup/stop is marked with stars. Since a gaussian distribution with zero mean is assumed, the exceedance probability for zero is equal to 0.5.

Wind speed [m/s]	Annual number of start up/stops	Gust from theory (Kaimal)[m/s]	Gust in IEC61400-1 [m/s]
5	1500	3.5	4.9
15	800	8.5	8.9
25	200	12.9	12.9

Table 3.1. Results of EOG model.

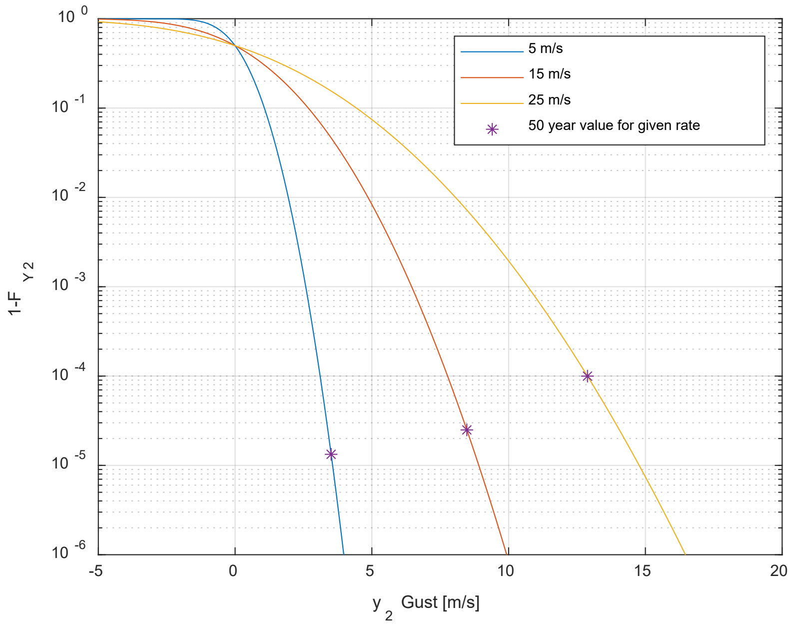

Figure 3.3. Probability of exceedance for gusts y_2 for Iref=0.16. The quantiles corresponding to a combined 50 year event with startup/stop is marked with stars.

Running the same calculations with other turbulence intensities, the same pattern is seen as shown in Figure 3.4, i.e. the same is obtained for the highest wind speed, whereas the IEC61400-1 gives conservative gust values for the lower wind speeds, with the assumed number of events,

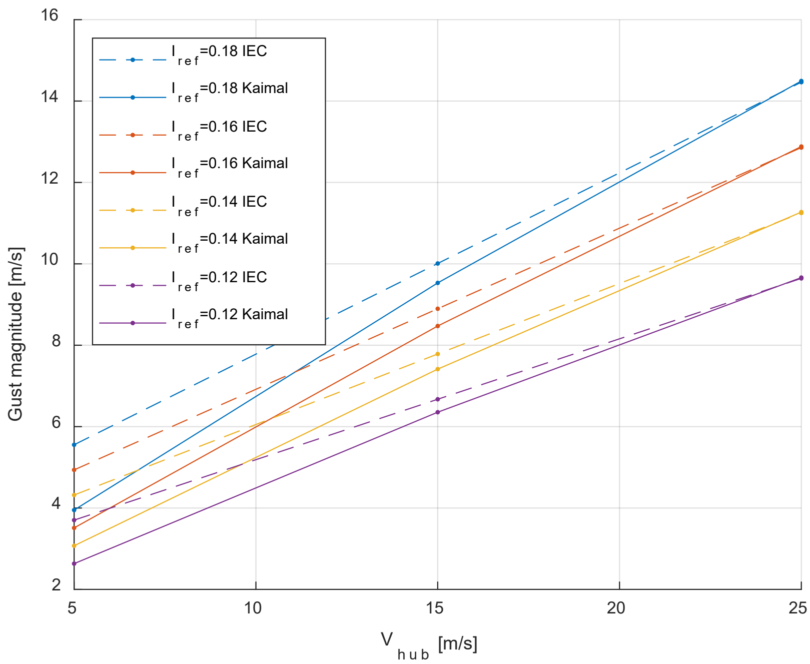

Figure 3.4. Gust magnitude based on IEC61400-1 and based on the Kaimal spectrum for turbulence intensities corresponding to class A+, A, B, and C.

To use the deterministic wind field event EOG for probabilistic design, the distribution for the annual maximum gust occurring together with an event is needed. For the DLCs with startup/stop the rates are high, and the probability of no events in a year is practically zero. Then, the distribution function for the annual maximum gust can be approximated well by:

$$F_{Y_2}(y_2) \approx F_{Y_2}(y_2|E)^{f_T} \tag{3.10}$$

The distributions for the annual maximum gust occurring together with a startup/stop is shown in Figure 3.5 together with the 50 year values, with coincides with the 0.98 quantile in the distributions for the annual maximum gust. Thus these distributions (or the approach to obtain them) can be used for the probabilistic modelling of DLC3.2 and 4.2.

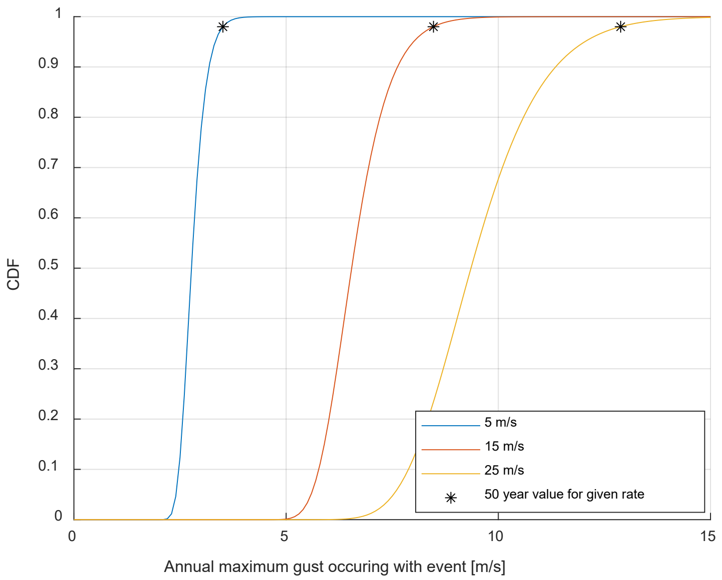

Figure 3.5. Distributions for the annual maximum gust occurring together with a startup/stop conditioned on Vhub and Iref=0.16.

DLC 2.3 (Electrical fault / loss of electrical network)

In DLC2.3, the same EOG wind profile as for DLC3.2 and 4.2 is used, but here together with the abnormal safety factor $\gamma_f = 1.1$ on the load effect instead of the normal safety factor $\gamma_f = 1.35$. Thereby, a rate of occurrence is not directly given; instead it is given implicitly through the safety factor. However, since the safety factor is applied on the load effect - not on the gust magnitude – the relationship depends on the wind turbine and the load effect. Here, the relation is investigated for the NREL 5MW onshore wind turbine. For rated wind speed 11.4 m/s and turbulence Iref=0.14, DLC 2.3 load simulations were performed with the deterministic wind field event EOG for five gust magnitudes, and this resulted in the relation shown in Figure 3.6.

In order to calculate the implicit rate of event for DLC2.3, we need to find the event frequency that results in the same design load when using a normal safety factor, as the current EOG load does when using the abnormal safety factor. Thus, the characteristic load should be reduced with a factor 1.1/1.35. From the relation between moment and gust magnitude, the required gust magnitude y_2 can then be found, as shown with a star in Figure 3.6. Using equation (3.8) and (3.9) and requiring $F_{Y_2}(y_2|E) = 1 - P_N$, the resulting quantile and event frequency can be obtained. For the given example, the exceedance probability was $P_N = 0.021$, and the corresponding event frequency is $f_T = 0.94$ per year.

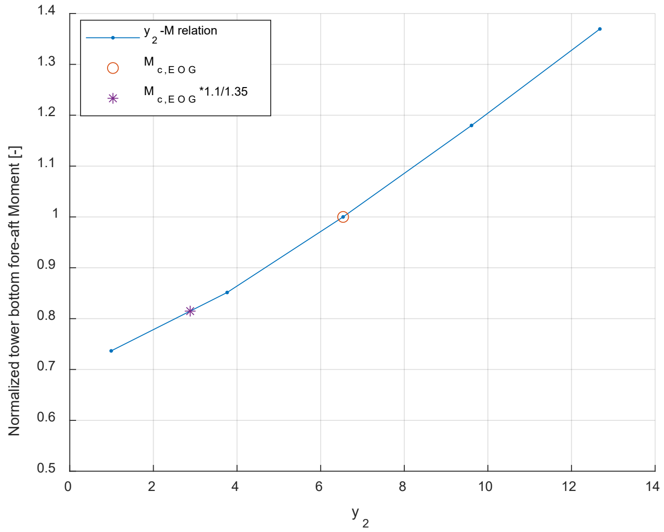

Figure 3.6. The characteristic value of extreme tower bottom fore-aft moment and the associated gust magnitude corresponding to an increased safety factor. Relation between the gust magnitude and the extreme tower bottom fore-aft moment. The moment is normalized with respect to the moment at the gust magnitude from IEC61400-1.

3.2.2 PROBABILISTIC GUST VIA FLOW ACCELERATION STATISTICS

To make a probabilistic version of "gusts" beyond the EOG in the IEC 61400-1 (Eds. 3–4), we can exploit long-term statistics of load-driving flow accelerations derived in the Hiperwind project [Kelly & Vanem, 2022; Kelly, 2023].

The EOG is defined such that its maximum implied acceleration is equal to $0.58V_{\text{gust}}/T_{EOG}$, where the IEC standard currently prescribes $T_{EOG} = 10.5\text{s}$, and V_{gust} for modern turbines is set in terms of the speed, reference turbulence intensity, and length scale Λ_1 (which is constant due to multi-megawatt turbine hub heights exceeding 60m), as noted with eq.3.7 above. But instead of presuming gusts to be related only to turbulence for a given wind speed, more generally and simply we can replace $0.58V_{\text{gust}}/T_{EOG}$ by the effective streamwise acceleration a_x which is sampled from its long-term distribution.

The EOG's "hat"-like shape can also be simplified and extended probabilistically to allow for distributions of gust duration (rise time), as well as acceleration or velocity jump amplitudes. A generalized shape function allowing such is

$$u(t) = U + \pi^{-1} a_x\, T_d \left\{1 + \tanh\left[\frac{\pi(t - t_0)}{T_d}\right]\right\} \tag{3.11}$$

where U is the pre-gust wind speed, a_x is the streamwise gust acceleration amplitude, T_d the event duration (rise time), and the optional parameter t_0 allows one to shift the gust in time. Figure 3.7 shows this gust form for three different values of T_d in Figure 3.7 all having a_x equal to that of the IEC's EOG form, which is also shown. Here $t_0 = 4$ s is used, to give the same time of maximum acceleration as in the EOG form.

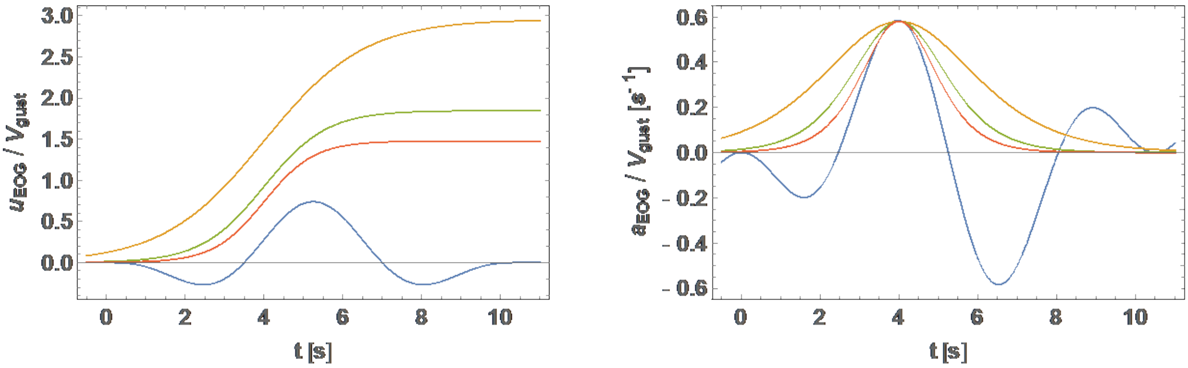

Figure 3.7. Normalized acceleration-based probabilistic gust form (left) and corresponding normalized acceleration (right). Three different rise-times depicted: 4 s (red), 5 s (green), and 8 s (gold). EOG prescription also shown in blue.

The amplitudes a_x chosen for the plots in Figure 3.7 correspond to commonly-observed values of accelerations observed at heights of 100–160m offshore [Kelly & Vanem, 2022, Kelly 2023].

The accelerations depicted and their distributions correspond to long-term statistics of 10-minute P_{99} of low-pass filtered accelerations, i.e., *load-driving* accelerations (this is detailed in Kelly & Vanem, 2022 and Kelly, 2023). The filter scale, corresponding to effective turbine response time, can be taken as 0.1 Hz; such a practical choice allows stochastic aeroelastic simulation of many gust events, some of which may be "filtered out" by the turbine, but which still excludes most of the events which are too short to affect turbine loads.
The tail of the long-term distribution of 10-minute P_{99} of low-pass filtered streamwise flow-accelerations can be represented as log-normal,

$$P(a) = \frac{1}{a\sigma_a\sqrt{2\pi}} \exp\left\{-\frac{1}{2}\left(\frac{\ln a - \mu_a}{\sigma_a}\right)^2\right\} ; \tag{3.12}$$

the form is such that the $\{\mu_a, \sigma_a\}$ actually correspond to the normal distribution which is exponentiated. On average, the expected acceleration-event duration (rise time) T_d for a given streamwise extreme flow acceleration has been empirically found (from both ramp and OWA studies as well as in Hiperwind) to follow $T_d \approx (6\text{ m/s})/a$. However, aside from longer ramps with insignificant accelerations, this is valid for accelerations $a_{\rm ref}$ with durations roughly shorter than the filter timescale f_c^{-1} (characteristic turbine response time); for practicality the truncated form

$$T_d \simeq \frac{(6\text{ m/s})/a_{\rm ref}}{[1+(a/a_{\rm ref})^3\,]^{1/3}} = \frac{(\Delta t)_{\max}}{[1+(a/a_{\rm ref})^3\,]^{1/3}} \tag{3.13}$$

Is recommended. To give a distribution of rise times Δt the T_d from (10) needs to be multiplicatively perturbed, given that Δt has also been observed to follow a log-normal distribution. For the range of wind speeds of relevance, i.e., from cut-in (~4m/s) to just beyond typical rated speed (~12–13 m/s), a dimensionless log-normal perturbation distribution of the form suffices.

$$\frac{1}{w\sqrt{2\pi}} \cdot \exp\left\{-\frac{1}{2}\left[w^2 + \left(\frac{\ln x}{w}\right)^2\right]\right\} \quad , \quad w = 0.2 \tag{3.14}$$

An example of the PDF's of 10^6 Monte-Carlo simulated values, using $a_{\mathrm{ref}} = 0.4\,\mathrm{m/s^2}$ and selecting $a > 0.3\,\mathrm{m/s^2}$, is shown below in Figure 3.8.

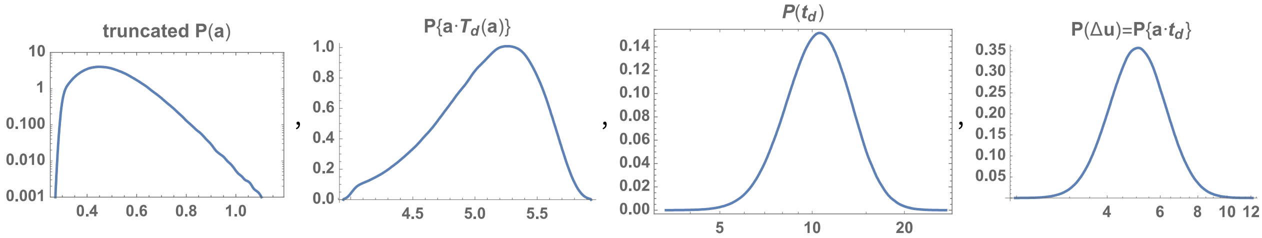

Figure 3.8. Distributions of gust acceleration amplitude, acceleration amplitude multiplied by nominal rise time, rise time, and wind speed amplitude (product of stochastic acceleration and stochastic rise time).

Over high surface roughness or complex terrain (e.g., forests, hills having elevation differences on the order of hub height, or RIX>5%), the load-driving acceleration statistics are affected more by the surface, and can differ from that shown here.

3.2.3 ALTERNATIVE MODELLING OF DLC 2.3

In addition to the EOG based model, IEC 61400-1:2019 has also suggested an alternative for DLC 2.3. Herein, DLC 2.3 may be modelled as a normal event, with partial safety factor for load = 1.35, assuming stochastic wind conditions and using the normal turbulence model, in combination with an electrical fault, including grid loss. For each mean wind speed considered, 12 simulations are carried out with different seeds. The fault is to be introduced into the simulation once the transient phase has subsided and the extreme response after the fault is sampled. For a particular mean wind speed, the nominal extreme response is evaluated as the mean of the 12 sampled extreme responses plus three times the standard deviation of the samples. The extreme response, from among the nominal values, is defined as the characteristic response for DLC 2.3.

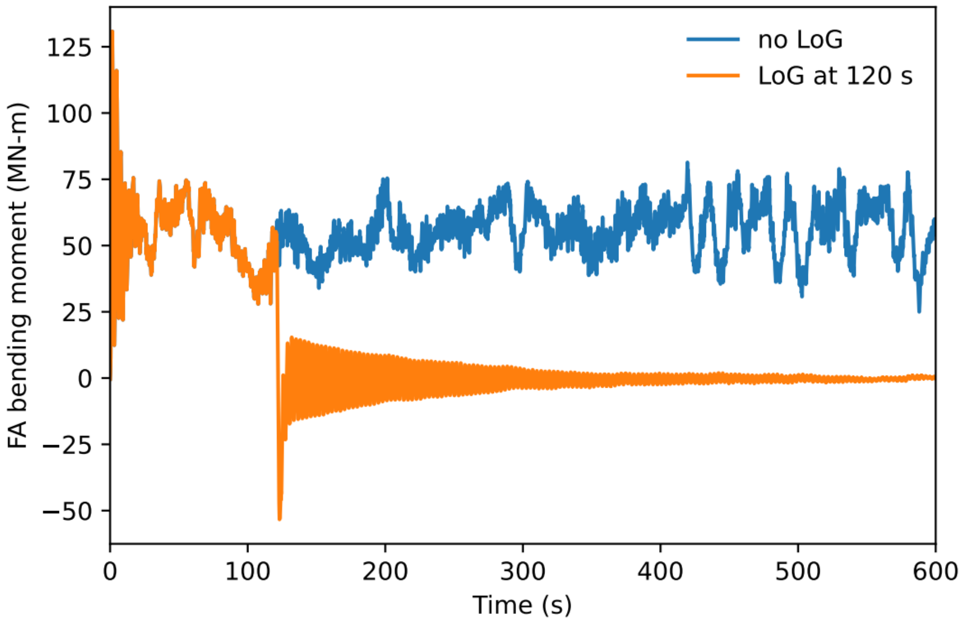

Figure 3.9 Turbine response under electrical fault

The response (fore-aft bending moment at the base of the tower) of the NREL 5MW land-based wind turbine under stochastic wind loading, when subjected to an electrical fault is shown in Figure 3.9. Here, the loss of grid (LoG) is introduced at 120 s after the start of the simulation, keeping in mind the transient response. The fault is simulated by pitching the blades to the feather condition, at the maximum pitch rate. The turbine shut down results in a sudden drop in thrust, accompanied by a damped oscillation of the tower. The maximum response is observed immediately after the introduction of the fault.

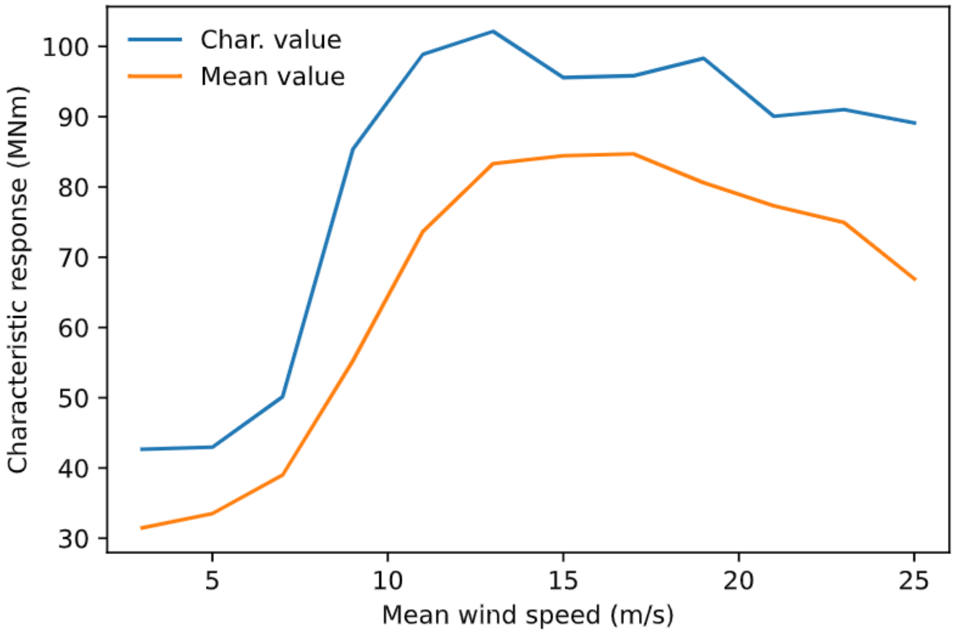

Figure 3.10 Characteristic load from NTM analysis

An illustration for DLC 2.3, using the alternate methodology presented in IEC 61400-1:2019 is shown in Figure 3.10. Aerodynamic simulations were performed in FAST, using the stochastic wind fields generated by TurbSim. 12 simulations are run for each wind speed from 3 m/s to 25 m/s, with a step of 2 m/s. For each simulation, the extreme value of the response after the electrical fault has occurred was sampled. For a particular mean wind speed, the extreme response was evaluated as the mean of the 12 sampled extreme responses plus three times the standard deviation of the samples, as shown in Figure 3.10.

3.3 BACKGROUND OF RELIABILITY LEVELS

The general standard for reliability of structures ISO2394 recommends to use economic optimization to derive optimal target reliabilities. If there is a risk of fatalities associated with a structural failure, minimum acceptable reliabilities can be found using the marginal lifesaving cost principle. In IEC61400-1 it is assumed that the risk to human lives can be neglected, as wind turbines are generally erected in remote locations.

Optimal target reliabilities are obtained by solving an optimization problem, where the net present value of the benefit minus the costs is maximized:

$$\boldsymbol{p}^* = \arg\max_{\boldsymbol{p}}\{Z(\boldsymbol{p})\} \quad (3.15)$$

$$Z(\boldsymbol{p}) = B(\boldsymbol{p}) - C(\boldsymbol{p}) - A(\boldsymbol{p}) - D(\boldsymbol{p}) - OM(\boldsymbol{p}) \quad (3.16)$$

where expected present values are used for:

- $B(\boldsymbol{p})$: benefit from existence of structure
- $C(\boldsymbol{p})$: construction cost
- $A(\boldsymbol{p})$: obsolescence cost
- $D(\boldsymbol{p})$: failure cost
- $OM(\boldsymbol{p})$: O&M costs

The reliability level and costs depend on the decision variables decision variables $\boldsymbol{p}$, which are related to e.g. the geometry of the structure, cross sectional parameters, and material strengths. Generally, a more reliable structure will be more expensive, and the optimal reliability represents a balance between these two competing costs.

The net present value of the benefits minus the costs are can be calculated based on an infinite or a finite time horizon. The infinite time horizon is appropriate for repairable components and for structures, where a new structure is erected in case of failure. Here, it is not necessary to include the benefit and O&M costs, if it does not depend on the design parameter (loss of benefit can be included in the failure costs). A finite horizon model is appropriate if a new structure is not erected in case of failure. In this case, the benefit and O&M costs are included, as it is lost in the case of failure.

3.4 TARGET RELIABILITIES BASED ON ECONOMIC OPTIMIZATION FOR STRUCTURES – SYSTEMATIC RECONSTRUCTION

The approach for economic optimization for new structures was considered by [Rackwitz 2000], and in Table 3.2 the derived target reliabilities are given. The background for the table was elaborated by [Fischer et al 2019].

Relative cost of safety measure	Consequence of failure		
	Minor	Moderate	Large
Large (A)	$\beta = 3.1$ ($P_f \approx 10^{-3}$)	$\beta = 3.3$ ($P_f \approx 5 \cdot 10^{-4}$)	$\beta = 3.7$ ($P_f \approx 10^{-4}$)
Normal (B)	$\beta = 3.7$ ($P_f \approx 10^{-4}$)	$\beta = 4.2$ ($P_f \approx 10^{-5}$)	$\beta = 4.4$ ($P_f \approx 5 \cdot 10^{-6}$)
Small (C)	$\beta = 4.2$ ($P_f \approx 10^{-5}$)	$\beta = 4.4$ ($P_f \approx 5 \cdot 10^{-6}$)	$\beta = 4.7$ ($P_f \approx 10^{-6}$)

Table 3.2. Optimal annual target reliabilities, β and annual failure probabilities, P_f based on economic optimization.

As decisions are made for a fleet of structures in relation to standardization, systematic reconstruction after failure and obsolescence is assumed, i.e. it is assumed that it is possible to erect new wind turbines at the site. Failure events and obsolescence events are assumed to occur randomly in time with rates λ and ω. Only costs to construction, obsolescence and failure are included, as the other costs are assumed independent of the decision variables $\boldsymbol{p}$ which determine the reliability level. The O&M costs are assumed independent of the decision variables. The optimal values of the decision variables $\boldsymbol{p}$ are found by maximizing the net present value of the benefit minus the costs for an infinite time horizon:

$$\boldsymbol{p}^* = \arg\max_{\boldsymbol{p}}\{Z(\boldsymbol{p})\} \tag{3.17}$$

$$Z(\boldsymbol{p}) = B(\boldsymbol{p}) - C(\boldsymbol{p}) - A(\boldsymbol{p}) - D(\boldsymbol{p}) \tag{3.18}$$

The benefits from the existence of the structure are assumed independent of $\boldsymbol{p}$, thus $B(\boldsymbol{p}) = B$. Therefore, the benefit needs not to be considered in the analysis, and instead the minimum of the expected net present value of the costs is found, thus the objective function becomes:

$$T(\boldsymbol{p}) = C(\boldsymbol{p}) + A(\boldsymbol{p}) + D(\boldsymbol{p}) \tag{3.19}$$

Costs occurring in the future should be discounted. Continuous discounting is performed by multiplication by $\exp(-\gamma t)$, where γ is the interest rate. The cost of first construction $C(\boldsymbol{p})$ occur at time zero and should not be discounted. The expected present value of the obsolescence costs $A(\boldsymbol{p})$ is calculated from additional reconstructions occurring with constant obsolescence rate ω:

$$A(\boldsymbol{p}) = \int_0^\infty \exp(-\gamma t) \cdot \omega \cdot C(\boldsymbol{p}) dt = C(\boldsymbol{p})\frac{\omega}{\gamma} \tag{3.20}$$

The expected present value of the failure costs $D(\boldsymbol{p})$ is found by assuming a constant failure rate $\lambda(\boldsymbol{p})$, and by accounting for additional failure costs H in addition to the reconstruction costs:

$$D(\boldsymbol{p}) = \int_0^\infty \exp(-\gamma t) \cdot \lambda(\boldsymbol{p}) \cdot (C(\boldsymbol{p}) + H) dt = (C(\boldsymbol{p}) + H)\frac{\lambda(\boldsymbol{p})}{\gamma} \tag{3.21}$$

The present value of the total costs are then:

$$T(\boldsymbol{p}) = C(\boldsymbol{p}) + C(\boldsymbol{p})\frac{\omega}{\gamma} + (C(\boldsymbol{p}) + H)\frac{\lambda(\boldsymbol{p})}{\gamma} \tag{3.22}$$

A single decision parameter p is defined as the central safety factor between the expected values of resistance *R* and load effect *S:*

$$p = \frac{E[R]}{E[S]} \tag{3.23}$$

The construction costs are assumed to be comprised by a term proportional to p, and a constant term:

$$C(p) = C_0 + C_1 p \tag{3.24}$$

The failure rate $\lambda(p)$ is estimated as the annual probability of failure, $P_f(p)$, which can be found using structural reliability methods for known distributions for resistance and annual maximum load effect:

$$\lambda(p) \approx P_f(p) = P[R - S < 0] \tag{3.25}$$

The total expected present value of the costs can be written as*:*

$$T(p) = (C_0 + C_1 p)\left(1 + \frac{\omega}{\gamma}\right) + (C_0 + C_1 p + H)\frac{P_f(p)}{\gamma} \tag{3.26}$$

Then, the optimal target annual reliability β^* is found from minimizing *T(p)* wrt. *p:*

$$p^* = \arg\min_p\{T(p)\} = \arg\min_p\left\{(C_0 + C_1 p)\left(1 + \frac{\omega}{\gamma}\right) + (C_0 + C_1 p + H)\frac{P_f(p)}{\gamma}\right\} \tag{3.27}$$

$$\beta^* = -\Phi^{-1}\left(P_f(p^*)\right) \tag{3.28}$$

In [Fischer et al 2019], the optimal reliabilities are found for ranges of the relative marginal safety costs C_1/C_0 and relative failure consequences H/C_0:

C_1/C_0: relative cost of safety measure:

A. Large: $10^{-2} \leq \frac{C_1}{C_0} \leq 10^{-1}$
B. Normal: $10^{-3} \leq \frac{C_1}{C_0} \leq 10^{-2}$
C. Small: $10^{-4} \leq \frac{C_1}{C_0} \leq 10^{-3}$

$H/C_0 \approx \rho - 1$: relative failure consequences

1. Minor: $\rho < 2$: $H/C_0 \leq 1$
2. Moderate: $2 \leq \rho \leq 5$: $1 \leq H/C_0 \leq 4$
3. Large: $5 \leq \rho \leq 10$: $4 \leq H/C_0 \leq 9$

Additionally, the optimal reliabilities depends on obsolescence rate ω, interest rate γ, and distribution types and coefficient of variation for resistance and load effect through $P_f(p) = P[R - S < 0]$. Table 3.2 can be obtained using $\omega = 0.02$, $\gamma = 0.03$, and lognormal distributions for R and S with coefficient of variation equal to 0.3.

Figure 3 can be obtained using $C_0 = 1$, $C_1 = 5 \cdot 10^{-2}$ and $H = 1$.

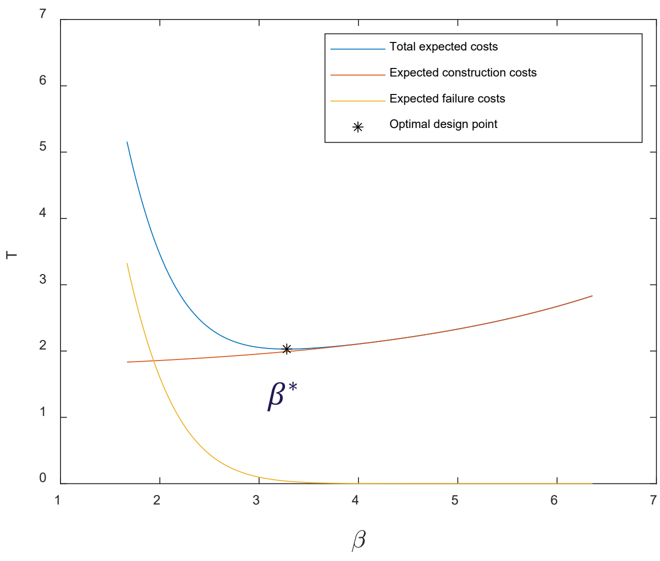

Figure 3.11. Total expected costs T as function of annual reliability index β for the base case with the optimal target reliability β^*.

3.4.1 PARAMETER STUDY

This section aims to illustrate the effect of changing the input parameters. Figure 3.12 shows the effect of changing the relative costs of increasing reliability $\frac{C_1}{C_0}$ and the relative costs of failure $\frac{H}{C_0}$. When C_1 is increased, the slope of the construction cost contribution is increased, and the target reliability is decreased. When H is increased, the negative slope of the failure cost contribution is increased, and the target reliability is increased.

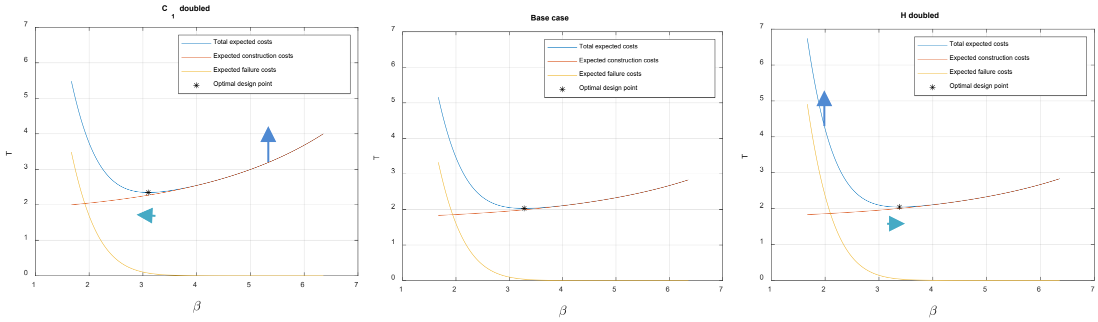

Figure 3.12. Total expected costs T as function of annual reliability index β.

Figure 3.13 shows the effect of changing the relative costs of increasing the obsolescence rate ω and interest rate γ. When ω is increased, the slope of the construction cost contribution is increased, and the target reliability is decreased. When γ is increased, the slope of both contributions are decreased, but the failure cost contribution is affected the most, and consequently, the target reliability is decreased.

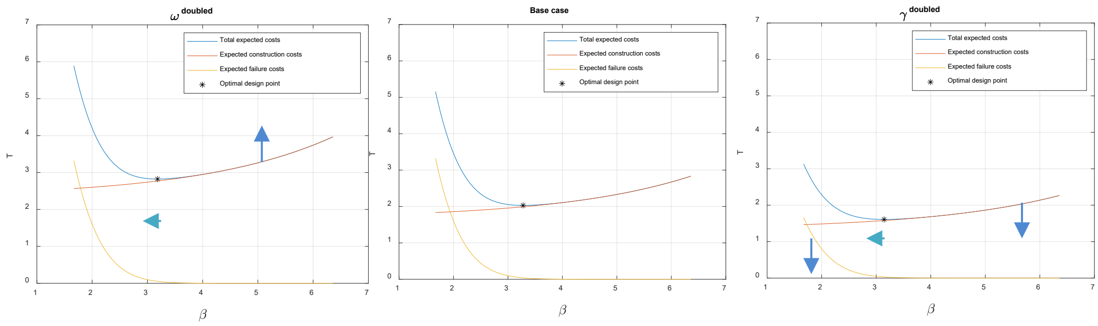

Figure 3.13. Total expected costs T as function of annual reliability index β.

Figure 3.14 shows the effect of changing the relative costs of the uncertainty of the load S. Increasing the COV, increases the slope of the construction cost contribution, and reduce the target reliability, and vice versa if the COV is decreased. A similar effect can be obtained by increasing the COV of the resistance. It should be noted that this model assumes the limit states for different years to be independent, which imply that there are no time-invariant uncertainties. In reality, uncertainties related to the resistance and model uncertainties on the load are typically time-invariant.

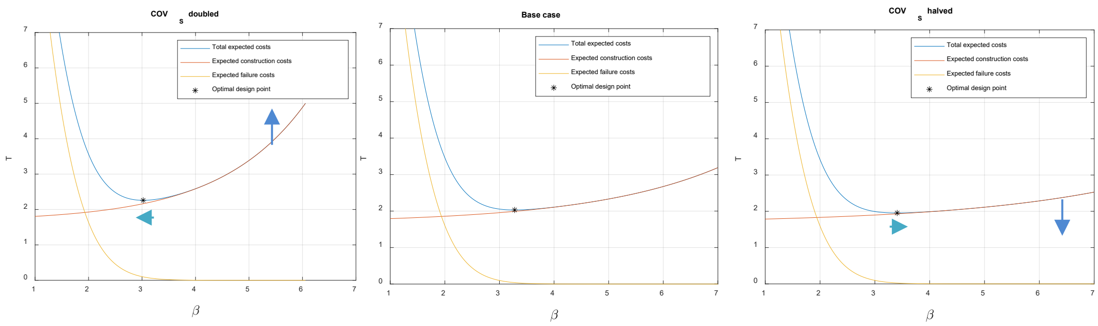

Figure 3.14. Total expected costs T as function of annual reliability index β.

3.5 TARGET RELIABILITIES – NO RECONSTRUCTION AFTER FAILURE

In this section, target reliabilities are derived for components that are not reconstructed in case of failure; this will often be the case for major failures leading to total collapse of the wind turbine. In this case, computations are performed for a finite lifetime, and the benefits and O&M costs are included, as they will be affected by a failure. The model is similar to a model derived for life extension of wind turbines [Nielsen & Sørensen, 2021]. The model allows for considering any distribution for the time to failure, thus a constant failure rate is not assumed here. The target reliability is defined based on the lowest annual reliability level in the planned lifetime. For fatigue failure, this is typically the last year of operation, and for extreme loads, this will be the first year.

The optimal design parameter (and thereby reliability $\beta(p)$) is found by maximization of the expected present value of the profit (benefits minus costs):

$$Z(p) = B(\beta(p)) - C(p) - OM_1(\beta(p)) - OM_2 - D(\beta(p)) \tag{3.29}$$

with expected present values of:

- $B(\beta(p))$: benefits
- $C(p) = C_0 + pC_1$: construction costs
- $OM_1(\beta(p))$: variable O&M costs
- OM_2: fixed O&M costs
- $D(\beta(p))$: failure costs / consequences
- $\beta(p)$: largest reliability index during the planned life

In case of a failure, the costs are affected as shown in Figure 3.15. Figure 3.15a shows the distribution of costs and benefits over the lifetime if there is no failure. In the case of a failure, the costs are affected, and Figure 3.15b shows the distribution of costs in case of a failure in year 7. The expected present value of benefits, variable O&M costs and failure costs depends on the distribution for the time to failure, and can be evaluated based on equations presented in [Nielsen & Sørensen, 2021].

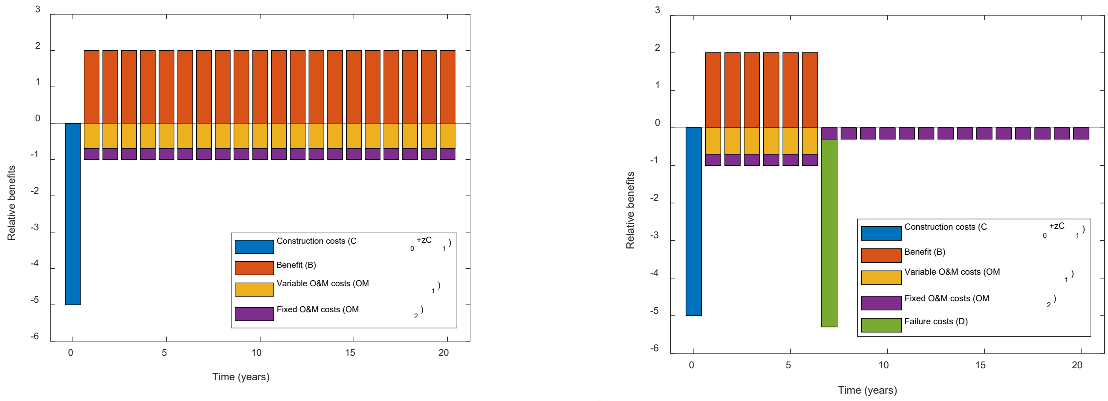

a b

Figure 3.15. Cost distribution if no failure and cost distribution if failure in year 7.

The cost model is defined by the following specific costs:

- Annual benefits: b
- Annual O&M costs: c_{OM}
- Proportion of O&M costs that are variable: OM_{var}
- Basic construction costs: C_0
- Costs of increasing z: C_1
- Failure consequences: H

3.5.1 BASIC COST MODEL

A basic cost model is defined to include only parameters affecting the reliability target the most. Based on initial studies it is found that the loss of benefits in case of failure is dominating compared to direct failure consequence. The following assumptions are made:

- Only relative costs are important therefore: $b - c_{OM} = 1$
- The proportion of O&M costs that are variable is of minor importance: $OM_{var} = 1$
- Basic construction costs do not affect optimum: $C_0 = 0$
- The direct failure costs are disregarded: $H = 0$
- The only remaining cost variable is C_1

The basic cost model is illustrated in Figure 3.16.

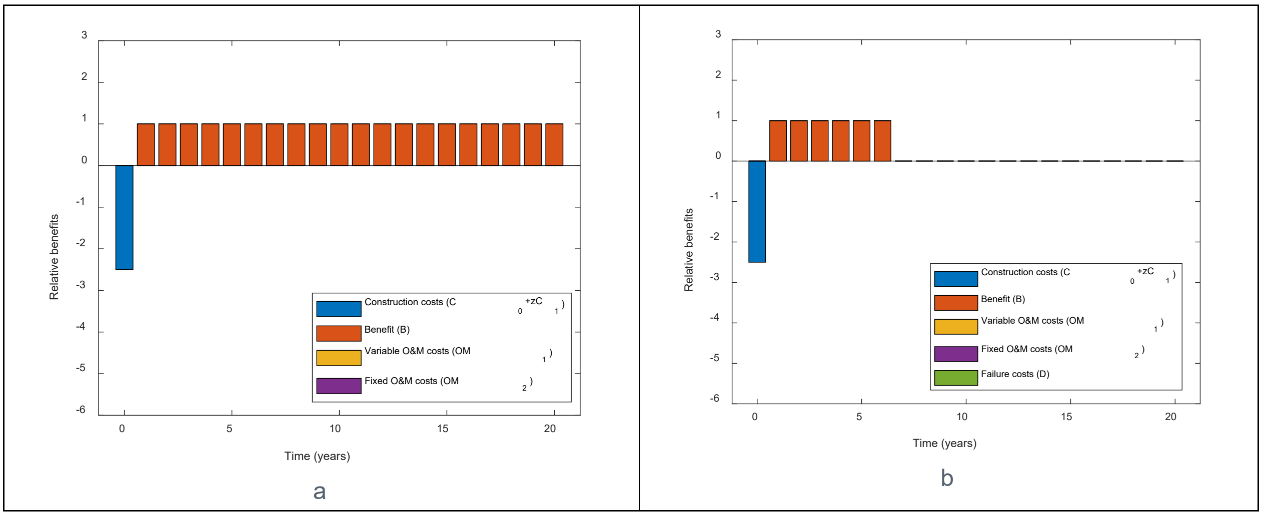

Figure 3.16. Basic cost model.

3.5.2 TIME TO FAILURE DISTRIBUTION FOR EXTREME LOADS

Often, the limit state equation for extreme loads is defined without time dependence. This is sufficient to evaluate the maximum annual failure probability. However, to calculate the time to failure distribution, the time dependence must be considered.

If failures occurred with constant rate (a Poisson process), the time to failure distribution would be given by the exponential distribution, which is decreasing with time. When time is discretized, this will be a Bernoulli process, and the time to failure distribution is a geometric distribution. The probability that failure happens in the second year is smaller than for the first year, because it cannot fail in the second year if it already failed in the first year. For the present stochastic model, the failure events are dependent through the time-invariant stochastic variables. This gives a further decrease in the failure probability, as each year with survival can be seen as a proof loading event, and only the realizations that survived the proof load, can potentially fail in later years. The probability of failure is therefore calculated as $P(g_t < 0 \cap \boldsymbol{g_{t-1}} > 0)$, i.e. the joint probability of failure in year t and survival in years up until year t. Based on Crude Monte Carlo simulations, where a new realization of the load is drawn for each year, this failure probability can be evaluated by identifying the year of the first failure in each simulated life.

Alternatively, an expression can be derived using linearized failure margins for the failure event for each year. Following [Thoft-Christensen and Sørensen, 1982] [Straub & Der Kiureghian, 2011], the probability of exactly x failures out of n elements is given by:

$$P_X(x) = \binom{n}{n-x} \int_{-\infty}^{\infty} \phi(u) \left(\Phi\left(\frac{-\beta + \sqrt{\rho}\, u}{\sqrt{1-\rho}} \right) \right)^{x} \left(\Phi\left(\frac{\beta - \sqrt{\rho}\, u}{\sqrt{1-\rho}} \right) \right)^{n-x} du \qquad (3.30)$$

where β is the element reliability index, ρ is the correlation between elements safety margins, and ϕ and Φ are the density and distribution function of the standard normal distribution, respectively. This can be seen as a binominal model for Bernoulli trials that are correlated due to the correlation coefficient between safety margins ρ.

The same principle can be applied to find the probability that the first failure happens in a given year, as this is the corresponding geometric distribution based on correlated Bernoulli trials. The probability that the first failure happens in year x is consequently:

$$P_X(x) = \int_{-\infty}^{\infty} \phi(u)\, \Phi\left(\frac{-\beta + \sqrt{\rho}\, u}{\sqrt{1-\rho}}\right)\left(\Phi\left(\frac{\beta - \sqrt{\rho}\, u}{\sqrt{1-\rho}}\right)\right)^{x-1} du \tag{3.31}$$

where β is the reliability index in the first year and ρ is the correlation between failure margins for different years. For two safety margins, the correlation can be estimated as the dot product of the α-vectors. For two identical safety margins with each n stochastic variables an indicator vector is defined as:

$I_i = 1$ for variables that are fully correlated for the two safety margins

$I_i = 0$ for variables that are independent for the two safety margins

The correlation coefficient is then estimated based on the α-vector for the safety margin:

$$\rho = \sum_{i}^{n} \alpha_i^2 \cdot I_i \tag{3.32}$$

3.6 RISK-BASED ASSESSMENT OF THE RELIABILITY LEVEL FOR EXTREME LIMIT STATES IN IEC 61400-1

Based on this approach, a risk-based assessment of the reliability level for extreme limit states in IEC 61400-1 was published in [Nielsen et al 2023]. The target reliabilities and safety factors in the IEC61400-1 are shown together with the optimal values found in the study in Table 3.3.

Load case	Current target reliability β	Optimal target reliability β	Current safety factor γ_f	Optimal safety factor γ_f
DLC 1.1 & 1.3	3.3	2.9	1.25 / 1.35	1.26
DLC 6.1	3.3	3.3	1.35	1.35
DLC 6.1 Typhoon	3.3	3.2	1.35 / 1.485	1.44
Gravity	3.3	3.4	1.10	1.12

Table 3.3. Optimal annual target reliabilities and load safety factors [Nielsen et al 2023].

For DLC 1.1, it was found that the annual reliability index is below the target β=3.3 due to the lower safety factor for this DLC (γ_f=1.25 instead of γ_f=1.35) compared to other load cases with extreme loads. However, for DLC 1.1 the resistance and model uncertainties dominate causing the correlation between limit states for different years to be large. Consequently, the cumulative reliability index is not larger than for the other load cases, and the average reliability index is larger than 3.3. The optimal value of the annual reliability index was found to β=2.9, which corresponds to the value found using the current load safety factor in IEC61400-1.

For DLC 6.1 with typhoon loads, the annual reliability index was found to β=3.1, when the normal load safety factor γ_f=1.35 was used. This will typically reflect the design, as the typhoon class was introduced in IEC 61400-1 ed. 4 without requirements to use increased safety factors. However, when using the optional increased safety factor given in a footnote in IEC 61400-1, the annual reliability index was larger than 3.3. For the typhoon case, the load uncertainty dominates, whereby the correlation coefficient between years is low. Therefore, the average reliability index is close to the annual reliability index in the first year, and the cumulative reliability index is low. The optimal annual reliability index is found to be only slightly lower than 3.3, and a larger load safety factor around 1.44 is needed to achieve this. However, this assumes that the costs of increasing the resistance is linear. If the demands for a resistance sufficient for typhoon loads require more radical design changes (resulting in a larger factor C_1/C_P), this could motivate a lower target reliability and a lower safety factor could be sufficient.

For the DLCs where it is found that the reliability implicitly given through the safety factors is less than the target β=3.3, the use of probabilistic methods directly with the target β=3.3 may lead to a more expensive design. If the target reliability level was in fact optimal based on economic risk-based considerations, then this more expensive design was in fact more optimal, because it gives the optimal balance between the failure risks and the costs of improving the reliability. However, we have demonstrated through a relative risk-based comparison between different load cases with extreme loads that a lower target reliability could be motivated for DLC 1.1, and this would correspond to the reliability level implicitly given through the safety factors in IEC 61400-1.

Therefore, a lower annual target reliability could also be used for probabilistic design according to IEC TS 61400-9 for DLC 1.1. This could be formulated as a reduced annual target reliability, as a lifetime reliability index, or it could be allowed to compare the average annual reliability index with the current target. It seems preferable to continue using annual target reliabilities, as they are least sensitive to the design lifetime. A reduced target for the annual failure probability would be easiest for the designer, as they would just need to calculate the annual failure probability. From a theoretical perspective, the most direct would be to allow the target to be compared to the average annual reliability index, corresponding to the asymptotic renewal density as suggested originally by [Rackwitz, 2000].

However, challenges arise in relation to through-life integrity management, where the reliability can be updated continuously based on inspections and monitoring data, and where decisions can be made related to operations and maintenance. Potentially, the use of a reduced target in this context, could lead to decisions that are not optimal, and this aspect should be considered carefully.

3.7 TARGET RELIABILITY LEVEL FOR SEISMIC SITES

In this section the target reliability level for seismic sites is considered and compared to non-seismic sites. The following representative stochastic model and optimization model for sites where seismic loads may be important are based on [Streicher & Rackwitz, 2006] and [Sørensen, 2021] where details of the models are presented.

Earthquakes are assumed to be modelled by a Poisson model with rate λ and magnitude M following a truncated Weibull distribution function. The probability density function of the peak ground acceleration A is modelled by $f_A(a)$. The following representative values from [Streicher & Rackwitz, 2006] are used: the coefficient of variation of the peak ground acceleration, V_A = 1.55 and the coefficient of variation of the response conditional on peak ground acceleration, Lognormal distributed with coefficient of variation V_S = 0.6.

A generic limit state equation is considered:

$$g = R - S \times A \times E \qquad (3.33)$$

where *R* is the resistance assumed to be lognormal distributed with coefficient of variation V_R. *S* is assumed lognormal distributed with coefficient of variation V_S. *E* is a model uncertainty assumed to be lognormal distributed with coefficient of variation V_E = 0.6. Assuming that the mean values of *S* and *E* are equal to 1 and a design parameter *p* is chosen equal to the mean value of *R* the conditional probability of failure given a peak ground acceleration a is obtained from the fragility curve:

$$P_f(p|a) = \Phi\left(-\frac{\ln\left(\frac{p}{a}\sqrt{\frac{(1+V_S^2)(1+V_E^2)}{(1+V_R^2)}}\right)}{\sqrt{(1+V_R^2)(1+V_S^2)(1+V_E^2)}}\right) \tag{3.34}$$

where $\Phi()$ is the standard Normal distribution function.

Next, a cost-based objective function excluding loss of human lives is considered, see [Streicher & Rackwitz, 2006]:

$$T(p) = C(p) + E_A\left[\left(C_R(p,a)\left(1-P_f(p|a)\right)\frac{\lambda}{\gamma}\right) + \left(C(p) + H_0 + H_M(a)\right)\frac{\lambda\, P_f(p|a)}{\gamma}\right] \tag{3.35}$$

where γ is the rate of interest, $C(p) = C_0 + C_1 p^{\delta}$ is the construction cost,

- $C_R(p,a) = C(p)(1 - \exp -0{,}25\, a)$ is the retrofitting cost,
- $H_M(a) = H_{M0} a^{o.4}$ is the physical damage cost and
- $H_0 = \ell C_0$ is the indirect cost of business

Typical relative values of the constants relevant for civil engineering structures are, see more details in [Streicher & Rackwitz, 2006]:

- C_0 = 10^6 modelling the basic costs,
- C_1 = 3 10^4 modelling the cost of safety measures,
- δ = 1.1,
- H_{M0} = 5 10^5,
- γ = 0.02,
- ℓ = 1.0 modelling the indirect costs

The optimal design parameter p^* is found solving $\min_p T(p)$ and the corresponding target annual probability of failure is obtained from $P_f^* = \lambda \int_0^{\infty} P_f(p^*|a)\, f_A(a)\, da$.

Without including costs related to loss of human lives the following results are obtained, see also (Sørensen, 2022):

V_R	C_1/C_0	ℓ	λ	$H_0 + E[H_M(a)]/C_0$	p^*	P_f^*
0.2	0.03	1.0	0.02	1.2	3.0	$13\ 10^{-4}$
0.2	0.03	1.0	0.05	1.2	2.7	$17\ 10^{-4}$
0.2	0.03	0.5	0.02	0.7	2.9	$16\ 10^{-4}$
0.2	0.03	4.0	0.02	4.2	3.8	$7\ 10^{-4}$
0.2	0.1	1.0	0.02	1.2	2.1	$32\ 10^{-4}$
0.1	0.03	1.0	0.02	1.2	2.9	$13\ 10^{-4}$

Table 4. Optimal design parameters and probability of failures.

It is seen that the results indicate that a larger target probability of failure for seismic load cases can be accepted compared to non-seismic areas; if the relative cost of safety measure is large then a larger target probability of failure can be accepted; the level of uncertainty of the resistance is not important since the uncertainty on the load side dominate. These observations are in line with the target reliability levels in the Eurocodes where a larger target probability of failure is accepted for seismic regions compared to non-seismic areas.

4 EXAMPLES AND BASELINE CALCULATIONS

4.1 DISCUSSION ON UNCERTAINTY QUANTIFICATION

Uncertainty quantification (UQ) examines the impact of model inputs on the variability of outputs, using probabilistic methods. UQ analysis involves two primary stages: uncertainty characterization and uncertainty propagation. In the first stage, uncertainty characterization, model inputs are described using probability distributions. Subsequently in the second stage, uncertainty propagation, the variability in model inputs is propagated through the model to determine the uncertainty in the outputs. This process often requires significant computational resources and time.

The uncertainties in the inputs can be classified as either aleatoric or epistemic. Aleatoric uncertainties arise from inherent randomness and cannot be reduced, such as wind speed, turbulence, wave height and frequency, current speed and direction, and earthquake magnitude. On the other hand, epistemic uncertainties stem from a lack of knowledge or data limitations and can be reduced when new information becomes available. Examples of epistemic uncertainties include reference turbulence intensity (an environmental condition variable), aerodynamic models, and joint distribution models for wind parameters.

When doing uncertainty quantification and propagation, it is imperative to properly characterize the joint probability distributions of the inputs, particularly when there are dependencies among them, as these dependencies significantly impact UQ outcomes. A common way of fitting probability distributions is the Maximum Likelihood method. In case the data are insufficient or for other reasons the true distributions cannot be estimated accurately, additional information can be combined with limited data through the use of Bayesian methods. The following sections 4.2 and 4.3 describe uncertainty quantification using Bayesian methods and using the maximum likelihood method respectively. A comparison of methods for model uncertainty quantification is published in [Nielsen 2023].

A common uncertainty propagation methodology involves using Monte Carlo simulation (MCS), where random samples are drawn from input probability distributions and propagated through the model to estimate output distributions. Employing MCS may necessitate a large sample size, posing computational challenges that can be burdensome or even unattainable. To enhance computational efficiency, practitioners often turn to surrogate models. Additionally, advanced sampling techniques like Latin hypercube sampling and pseudo-random methods such as Sobol and Halton sequences may be adopted. These techniques serve to fill the input space more uniformly, leading to the training of more accurate surrogate models. An example uncertainty propagation study assuming known joint distribution of the uncertainties and utilizing a surrogate modelling technique together with a Monte Carlo Simulation is shown in Section 4.4 of this document.

4.2 BAYESIAN METHODS FOR UNCERTAINTY QUANTIFICATION

Bayesian methods can be seen as the most general and consistent approach for uncertainty quantification. It allows for the combination of new data with existing information, and it allows for hieratical modelling of uncertainties. The theoretical description is generic and can be applied to all hierarchies and distribution types.

Bayes rule states that the posterior distribution $P(\theta|\varepsilon)$ of a variable is proportional to the product of the prior distribution $P(\theta)$ and the likelihood function $P(\varepsilon|\theta)$:

$$P(\theta|\varepsilon) \propto P(\theta) \cdot P(\varepsilon|\theta) \tag{4.1}$$

Here θ is a variable, and ε is the data or *evidence* available for updating/estimating the distribution for θ.

While Bayes rule holds for all distribution types, closed form solutions can only be found for specific combinations of prior and likelihood functions; the so-called conjugate distributions. An example is the normal distribution. If both the prior and likelihood distributions are normal distributions, the posterior distribution is also a normal distribution, and a closed form solution can be found. For hieratical models with normal distributions, where other variables are described as linear combinations of normal distributions, exact solutions can be found for the posterior distributions. For discrete distributions, exact solutions can also be derived. However, for arbitrary choices of continuous distributions, exact solutions cannot be found for the posterior distributions. Instead sampling based methods can be applied, or the continuous parameters can be discretized. For hieratical models, graphical models such as Bayesian networks are especially suitable.

When comparing Bayesian methods to other methods for estimation of parameters, Bayesian methods have the advantage, that existing information can be accounted for in the prior. However, Bayesian methods can also be used when no prior information is available, by using a non-informative prior: e.g. a uniform distribution over the range of the parameter or a normal distribution with a very high coefficient of variation.

4.2.1 CLOSED FORM SOLUTIONS FOR PARAMETER ESTIMATION

Closed form solutions exist for the predictive distribution of X for (among others) the following cases, where the population of X follows a normal distribution with unknown mean:

- Known population standard deviation (Figure 4.1a)
  - No prior information on the mean
  - Prior information on the mean
- Unknown population standard deviation (Figure 4.1b)
  - No prior information on the mean and standard deviation
  - Prior information on the mean and standard deviation

(a) (b)

Figure 4.1 Graphical representation of the structure for estimation of (a) the mean value of X when the population variance is known and (b) the mean value and the variance.

In addition to the prior information (if any) a new sample is available with sample size n, sample mean m, and sample standard deviation s:

$$m = \frac{1}{n}\sum_{i=1}^{n} x_i \tag{4.2}$$

$$s = \sqrt{\frac{1}{n-1}(x_i - m)^2} \tag{4.3}$$

The population of X follows a normal distribution with unknown mean and known/unknown standard deviation σ.

Known population standard deviation, no prior information
The predictive distribution for X is a normal distribution:

$$X'' = m + Z \cdot \sigma \sqrt{1 + \frac{1}{n}} \tag{4.4}$$

where Z follows a standard normal distribution. Note that for a large sample size *n*, $\sqrt{1 + \frac{1}{n}} \approx 1$, whereby X asymptotically approaches a normal distribution with mean and standard deviation equal to the sample values m and s.

Known population standard deviation, prior information
Prior information on the mean of X: normal distribution with sample with size n'). The predictive distribution for X becomes a normal distribution:

$$X'' = m'' + Z \cdot \sigma \sqrt{1 + \frac{1}{n''}} \tag{4.5}$$

where

- Z follows a standard normal distribution.
- $n'' = n' + n$
- $m'' = \frac{m'n' + mn}{n''}$

Unknown population standard deviation, no prior information

The predictive distribution for X is a student-t distribution:

$$X'' = m + T_{n-1} \cdot s\sqrt{1 + \frac{1}{n}} \qquad (4.6)$$

where T_{n-1} follows a student-t distribution with n-1 degrees of freedom. Note that for a large sample size n, the student-t distribution approximates a normal distribution and $\sqrt{1 + \frac{1}{n}} \approx 1$, whereby X asymptotically approaches a normal distribution with mean and standard deviation equal to the sample values m and s.

Unknown population standard deviation, prior information

The prior information on the mean and standard deviation of X is given by parameters m', v', s', n'. The prior for the mean is a normal distribution with mean $E[\mu] = m'$ and standard deviation $\sigma/\sqrt{n'}$ (corresponding to prior information originating from a sample with size n'). To obtain a conjugate prior for the standard deviation, the inverse of the squared standard deviation has a gamma distribution as prior, defined by the prior expected value of the standard deviation $E[\sigma] = s'$ and the prior degrees of freedom ν'. The prior degrees of freedom is related to the coefficient of variation of the standard deviation as follows: $COV[\sigma] = 1/\sqrt{2\nu'}$

The predictive distribution for X is a student-t distribution:

$$X'' = m'' + T_{\nu''} \cdot s''\sqrt{1 + \frac{1}{n''}} \qquad (4.7)$$

where

- $T_{\nu''}$ follows a student-t distribution with ν'' degrees of freedom
- $\nu = n - 1$
- $\nu'' = \nu' + \nu + 1$ for $n' \geq 1$ and $\nu'' = \nu' + \nu$ for $n' = 0$
- $n'' = n' + n$
- $m'' = \frac{m'n' + mn}{n''}$
- $s''^2 = (\nu' s'^2 + n' m'^2 + \nu s^2 + nm^2 - n'' m''^2)/\nu''$

Lognormal variable

If a variable X follows a lognormal distribution, $Y = \ln X$ follows a normal distribution. Therefore, the same approaches as above can be used for lognormal distributions, by making the inference on the logarithm of the variable.

For example, for the case with unknown population standard deviation and no prior information:

$$\ln X = m_{\ln X} + T_{n-1} \cdot s_{\ln X}\sqrt{1 + \frac{1}{n}} \qquad (4.8)$$

where

- T_{n-1} follows a student-t distribution with n-1 degrees of freedom
- $m_{\ln X}$ is the sample mean of $\ln(X)$

- $s_{\ln X}$ is the sample standard deviation of $\ln(X)$

The predictive distribution for X is then given by:

$$X = \exp\left(m_{\ln X} + T_{n-1} \cdot s_{\ln X}\sqrt{1+\frac{1}{n}}\right) = \exp(m_{\ln X}) \cdot \exp\left(T_{n-1} \cdot s_{\ln X}\sqrt{1+\frac{1}{n}}\right) \tag{4.9}$$

For small values of the coefficient of variance (less than 0.25), this can be approximated by:

$$X \approx m \cdot \exp\left(T_{n-1} \cdot COV_X\sqrt{1+\frac{1}{n}}\right) \tag{4.10}$$

where COV_X is the sample coefficient of variation of X.

4.2.2 EXACT INFERENCE FOR CONTINUOUS PARAMETERS

Exact inference can be performed for hierarchical models of normal distributions, where the top nodes follow normal distributions (prior distributions with given mean and variance), and the conditional probability distribution of the other nodes are normal distributions with mean values written as a linear combination of other normal distributed variables, and with known standard deviation. For variables that can be written as a product of lognormal distributed variables, the logarithmic transformation can be used, whereby the same approach can be used. Programs such as Hugin Expert can be applied.

4.2.3 SAMPLING BASED INFERENCE

For models with arbitrary continuous distribution types and relationships between parameters, sampling based methods such as Markov Chain Monte Carlo (MCMC) methods can be used. Top nodes are described by their prior probability distributions, and other nodes can be represented by deterministic functional relationships or by density functions, where other nodes can enter as distribution parameters. Nodes described functional relationships are referred to as logic nodes, whereas the other nodes are stochastic nodes. In a Markov Chain, the joint distribution of the simulated sample approximates the true joint distribution, when samples from the run-in period is discarded, and a sufficient number of samples is obtained. MCMC methods include families of algorithms such as Gibbs, Metropolis Hasting, and slice sampling. In Gibbs sampling, samples are drawn successively from the full conditionals of the stochastic nodes. The full conditional distribution for a node X is proportional to the to the product of the conditional distribution for X given the parents, and the conditional distributions for the child nodes of X, given their parents. For nodes with logic nodes as parents, the parents of the logic nodes are also included through the functional relationship. Gibbs sampling is performed by drawing samples from the full conditionals of the stochastic nodes in turn, conditioned on the most recent value of all other nodes. Samples are only drawn from stochastic nodes. If any of the nodes are observed, the values of these nodes are fixed to the observed values in the full conditionals. When MCMC methods are used for uncertainty quantification, the observations will typically be a sample with several (n) observations of an uncertain variable. Then n instantiations of the node are included in the network, which are independent and identically distributed.

Programs such as OpenBugs can be applied.

4.2.4 EXACT INFERENCE FOR DISCRETIZED PARAMETERS

For hieratical models with discrete distributions, where all distributions are given as (conditional) probability distributions, efficient algorithms exist for exact inference. The same method can be used for continuous distributions, by first discretizing the variables. Functional relationships can be approximated by conditional probability distributions. Programs such as Hugin Expert can be applied.

4.3 UNCERTAINTY QUANTIFICATION USING THE MAXIMUM LIKELIHOOD METHOD

An often used method for parameter estimation is the Maximum Likelihood method. Here, distribution parameters are estimated such that the probability of receiving the sample is maximized. For some distribution types, analytical closed form solutions exist for the maximum likelihood estimate of the parameters. For other distributions, optimization algorithms can be used to estimate the parameters, based on a sample. The statistical uncertainty (standard deviations and correlation coefficients) related to the estimated parameters can be estimated based on the hessian matrix (consisting of the second derivatives of the log-likelihood function in the point of maximum likelihood estimate).

The likelihood function is the product of the probability density function $f_X(x;\boldsymbol{\theta})$ evaluated in the *n* sample points, as function of distribution parameters $\boldsymbol{\theta}$:

$$L(\boldsymbol{\theta}) = \prod_{i=1}^{n} f_X(x_i;\boldsymbol{\theta}) \tag{4.11}$$

To ease the computations for analytical solutions and to avoid numerical underflow for numerical calculations, the loglikelihood function is used. When taking the natural logarithm of the likelihood function, the loglikelihood function is obtained:

$$LL(\boldsymbol{\theta}) = \sum_{i=1}^{n} \ln\left(f_X(x_i;\boldsymbol{\theta})\right) \tag{4.12}$$

The maximum likelihood estimate is found as the parameters maximizing $LL(\boldsymbol{\theta})$ (and thereby also $L(\boldsymbol{\theta})$). This can be done using numerical optimization algorithms or analytically from *j* equations:

$$\frac{\partial LL(\boldsymbol{\theta})}{\partial \theta_j} = 0 \tag{4.13}$$

The hessian matrix for three parameters θ_1, θ_2, θ_3 is given by:

$$\boldsymbol{H} = \begin{bmatrix} \frac{\partial^2 LL(\boldsymbol{\theta})}{\partial \theta_1^2} & \frac{\partial^2 LL(\boldsymbol{\theta})}{\partial \theta_1 \partial \theta_2} & \frac{\partial^2 LL(\boldsymbol{\theta})}{\partial \theta_1 \partial \theta_3} \\ \frac{\partial^2 LL(\boldsymbol{\theta})}{\partial \theta_1 \partial \theta_2} & \frac{\partial^2 LL(\boldsymbol{\theta})}{\partial \theta_2^2} & \frac{\partial^2 LL(\boldsymbol{\theta})}{\partial \theta_2 \partial \theta_3} \\ \frac{\partial^2 LL(\boldsymbol{\theta})}{\partial \theta_1 \partial \theta_3} & \frac{\partial^2 LL(\boldsymbol{\theta})}{\partial \theta_2 \partial \theta_3} & \frac{\partial^2 LL(\boldsymbol{\theta})}{\partial \theta_3^2} \end{bmatrix} \tag{4.14}$$

The covariance matrix is then given by:

$$\boldsymbol{C} = [-\boldsymbol{H}]^{-1} = \begin{bmatrix} \sigma_1^2 & \rho_{12}\sigma_1\sigma_2 & \rho_{13}\sigma_1\sigma_3 \\ \rho_{12}\sigma_1\sigma_2 & \sigma_2^2 & \rho_{23}\sigma_2\sigma_3 \\ \rho_{13}\sigma_1\sigma_3 & \rho_{23}\sigma_2\sigma_3 & \sigma_3^2 \end{bmatrix} \tag{4.15}$$

where σ_j is the standard deviation of parameter θ_j and ρ_{jk} is the correlation coefficient between parameter θ_j and θ_k.

The distributions for the parameters become asymptotically normal distributed (for more than 25-30 data) [Lindley 1965].

The same estimate as obtained using the maximum likelihood method can also be obtained using Bayesian inference, as the special case of Bayesian inference, where the prior distributions for the parameters are non-informative (uniform). The mode values of the parameter distributions (the value with highest probability) correspond to the maximum likelihood estimate.

4.4 EXAMPLE UNCERTAINTY PROPAGATION

This example focuses on the structural dynamic response model of the DTU 10MW reference wind turbine from the aero-servo-elastic simulation tool HAWC2 (Horizontal Axis Wind turbine simulation Code 2nd generation). The five model inputs are two wind parameters, ten-minute mean (u) and standard deviation (σ) of the wind speed in the longitudinal direction; the aerodynamic parameter lift coefficient (denoted as “cl"); and the structural parameters, the area moment of inertia for bending around the x (flapwise) axis of the blade (denoted as “blade Ix") and the fore-aft direction of the tower (denoted as “tower Ix"). The three model outputs are the three wind turbine responses: blade tower clearance (minimum distance between the blade tip and tower, denoted as “bTD"), blade root flap-wise moment Mx (maximum absolute value, denoted as “Mx blade"), and tower base fore-aft moment Mx (maximum absolute value, denoted as “Mx tower"). For each input set, there are 12 turbulence boxes with different random seeds, which leads to 12 different response outputs, the median of which is taken as the output.

The five input variables are shown in Table 4.1, where u is within the operational range of 3 m/s to 27 m/s. The cl, blade Ix, and tower Ix are in the form of profiles along the length of the blade or tower. The values in the ‘Range’ column represent a multiplier factor applied uniformly on the default profile. The range aims to cover the distributed range of each variable, e.g., the blade Ix follows Normal distribution with mean 1 and standard deviation 0.05, and the range [0.7,1.3] covers six standard deviations away from the mean.

Table 4.1 Distribution and range of input variables

Variable	Range	Distribution	Parameters
u	$[3, 27]$	Rayleigh	$\sqrt{2/\pi}\mathrm{V}_{ave}$
σ	$[\max(0, 0.1 \times (u-20)), 0.18 \times (6.8 + 0.75 \times u)]$	Weibull	$(0.27 \times u + 1.4, 0, \mathrm{I}_{ref} \times (0.75 \times u + 3.3))$
cl	$[0.7, 1]$	Half-Normal	$(1, 0.05/\sqrt{1-2/\pi})$
blade Ix	$[0.7, 1.3]$	Normal	$(1, 0.05)$
tower Ix	$[0.7, 1.3]$	Normal	$(1, 0.05)$

Ten thousand input sets are generated within the range specified in Table 4.1 using the Halton sequence. The Halton sequence is one of the low-discrepancy sequences (quasi-random number), which could fill the domain more evenly. Figure 4.2 compares a pseudo-random sample and a Halton sample with 1,000 data points in a two-dimensional space. The mean discrepancy from 100 sets of pseudo-random samples is $\sim 3.77 \times 10^{-4}$, and $\sim 2.07 \times 10^{-6}$ for Halton sequence.

The Sobol sequence and Latin Hypercube sampling could also be used, but finding the best sampling strategy is not the focus of this paper.

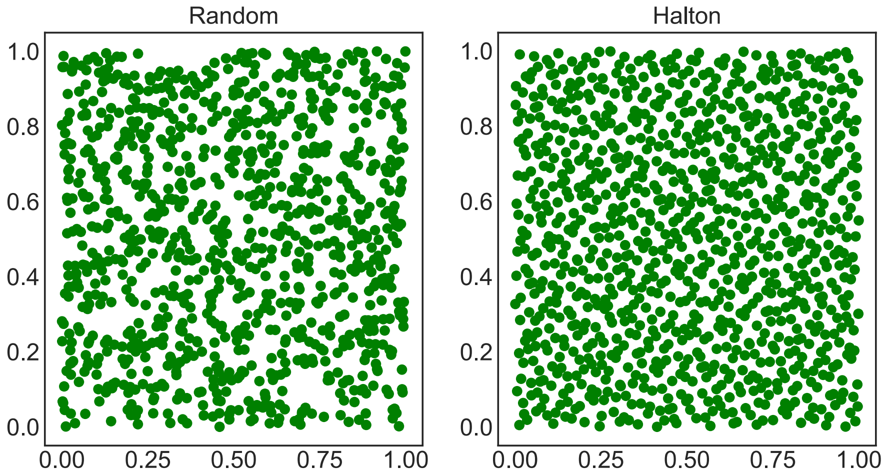

Figure 4.2 Comparison of the random sample and Halton sample

For each of the 10,000 variable sets, 12 random seeds are used for turbulence box generation. The time domain analysis with a 120,000 ($12 \times 10{,}000$) set of inputs is run using HAWC2.

A dataset comprising 10,000 input-output pairs serves as the training data for a surrogate model. To assess the model's accuracy, validation is conducted by partitioning the dataset into training and test sets. It's worth noting that the surrogate models can also find utility in tasks such as structural reliability analysis and global sensitivity analysis. For the purpose of evaluating the uncertainty in model outputs, a random sample is drawn based on the distribution outlined in Table 4.1. Subsequently, the corresponding responses are assessed using the surrogate models. The probability density functions of the wind turbine responses are visualized in Figure 4.3. The distribution of the wind turbine response exhibits a noteworthy feature: it is characterized by multiple modes. These outcomes illustrate how variations in input parameters contribute to output variability, offering valuable insights for design optimization. Furthermore, these results can be subjected to more in-depth analysis for applications such as structural reliability assessment or extreme load extrapolation. Additionally, a variance-based global sensitivity analysis can be employed to allocate the output variance to each individual input, providing a comprehensive understanding of the model's sensitivity to various factors.

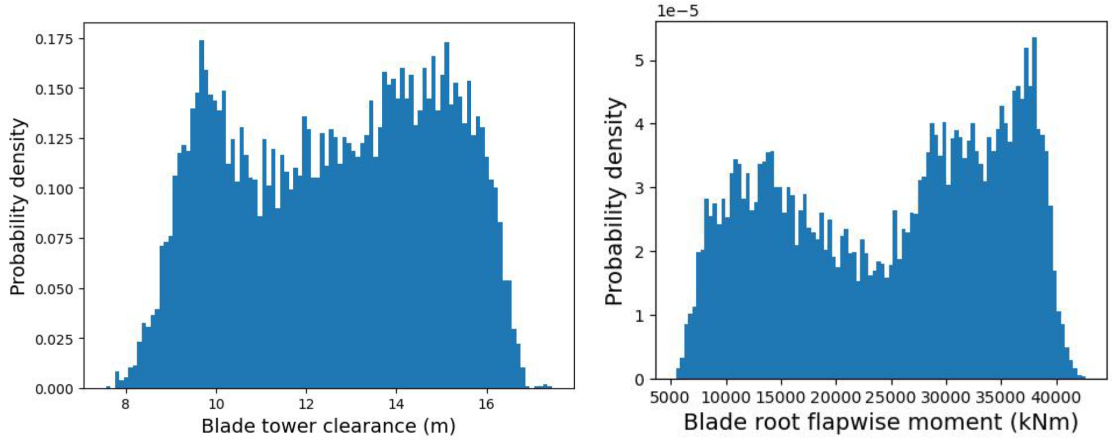

Figure 4.3 Propagated uncertainty distribution of wind turbine responses with respect to input uncertainties

5 REFERENCES

Abdallah, I.: Assessment if extreme design loads for modern wind turbines using the probabilistic approach. PhD Thesis, DTU Wind Energy PhD-0048, 2015.

Agarwal, P.: Structural Reliability of Offshore Wind Turbines. PhD thesis, University of Texas at Austin, 2008.

de las Heras, E.G., R. Gutiérrez, E. Azagra & J.D. Sørensen: Assessment of wind turbine for site-specific conditions using probabilistic methods. Proc. EWEA 2013.

Dimitrov, N. K., Natarajan, A., & Mann, J. (2017). Effects of normal and extreme turbulence spectral parameters on wind turbine loads. Renewable Energy, 101, 1180-1193. https://doi.org/10.1016/j.renene.2016.10.001

Dimitrov, N. K. (2020). Inverse Directional Simulation: an environmental contour method providing an exact return period. Journal of Physics: Conference Series, 1618(6), 062048. https://doi.org/10.1088/1742-6596/1618/6/062048

DNV-RP-C203:2021 Fatigue design of offshore steel structures

DNV-RP-C210:2021 Probabilistic methods for planning of inspection for fatigue cracks in offshore structures

DNV-ST-0126:2021 Support structures for wind turbines.

EN 1990:2002, Eurocode - Basis of structural design, European Committee for Standardisation

Fischer K, Viljoen C, Köhler J, Faber MH. Optimal and acceptable reliabilities for structural design. Struct Saf. 2019;76:149-161. doi:10.1016/J.STRUSAFE.2018.09.002

Hallowell, S.T. et al.: Hurricane risk assessment of offshore wind turbines. Renewable Energy, Vol. 125, September 2018, pp 234-249.

IEC 61400-1:2019, Wind Energy Generation Systems – Part. 1: Design requirements

IEC 61400-3-1: 2019 Wind energy generation systems – Part 3-1: Design requirements for fixed offshore wind turbines

ISO 2394:2015, General principles on reliability for structures, International Organization for Standardization

JCSS (2002). (Joint Committee on Structural Safety): Probabilistic Model Code. https://www.jcss-lc.org/

Lindley, D. V. (1965). Introduction to Probability and Statistics from a Bayesian Viewpoint. Cambridge University Press.

Madsen, H.O. & O. Ditlevsen: Structural reliability methods. John Wiley & Sons Ltd, Chichester, 1996.

Madsen, H. O., Krenk, S. & Lind, N.C. (1986). Methods of Structural Safety, Dover Publications, Inc.

Mardfekri, M. & P. Gardoni: Probabilistic demand models and fragility estimates for offshore wind turbine support structures. Engineering Structures, Vol. 52, 2013, pp 478-487.

Nielsen, J.S., & Sørensen, J.D. (2021). Risk-based derivation of target reliability levels for life extension of wind turbine structural components. Wind Energy, 1-18.

Nielsen, Jannie S., Comparison of methods for model uncertainty quantification, 14th International Conference on Applications of Statistics and Probability in Civil Engineering (ICASP14), Dublin, Ireland, 2023. http://hdl.handle.net/2262/103190

Nielsen, J.S.; Toft, H.S.; Violato, G.O. Risk-Based Assessment of the Reliability Level for Extreme Limit States in IEC 61400-1. *Energies* **2023**, *16*, 1885. https://doi.org/10.3390/en16041885

Quilligan, S., A. O'Connor & V. Pakrashi: Fragility analysis of steel and concrete wind turbine towers. Engineering Structures, Vol. 36, 2012, pp. 270–282.

Rackwitz R. Optimization — the basis of code-making and reliability verification. Struct Saf. 2000;22(1):27-60. doi:10.1016/S0167-4730(99)00037-

Sheng, C. & H.P. Hong: Reliability and fragility assessment of offshore floating wind turbine subjected to tropical cyclone hazard. Structural Safety, Vol. 93, 2021, pp. 102-138.

Stork, C. H. J., Butterfield, C. P., Holley, W., Madsen, P. H., & Jensen, P. H. (1998). Wind conditions for wind turbine design proposals for revision of the IEC 1400-1 standard. Journal of Wind Engineering and Industrial Aerodynamics, 74-76, 443–454.

Streicher, H. & R. Rackwitz: Optimization with a LQI Acceptance Criterion. Background Documents on Risk Assessment in Engineering - Document #5 - Optimization with a LQI Acceptance Criterion. JCSS Joint Committee of Structural Safety, 2006.

Sørensen, J.D. & Toft, H.S.: Safety Factors – IEC 61400-1 ed. 4 - background document. DTU Wind Energy-EReport-0066 (EN), 2014. https://vbn.aau.dk/da/publications/safety-factors-iec-61400-1-ed-4-background-document

Sørensen, J.D.: Probabilistic Design and Calibration of Partial Factors for Structural Systems. Proc. Int. Symp. on Emerging Developments and Innovative Applications of Reliability Engineering and Risk Managements (EDIARR2021), Chen, S. S. & Ang, Alfredo. H-S. (Eds), 2021.

Sørensen, J.D. & Toft, H.S. 2010. 'Probabilistic design of wind turbines'. Energies, Vol. 3, pp. 241-257. Veldkamp, D. 2006. 'Chances in Wind Energy – A Probabilistic Approach to Wind Turbine Fatigue Design'. PhD thesis, DUWIND Delft University, Wind Energy Research Institute, Delft.

Tarp-Johansen, N.J., Madsen, P.H. and Frandsen, S.T.: Calibration of Partial Safety Factors for Extreme Loads on Wind Turbines Proc. European wind energy conference and exhibition (EWEC), 2003.

Tarp-Johansen, N.J., P.H. Madsen & S. Frandsen: Partial safety factors for extreme load effects. RISØ-R-1319(EN), 2002.

Tarp-Johansen, N.J.: Partial safety factors and characteristic values for combined extreme wind and wave load effects. Journal of Solar Energy Engineering 2005, 127, 242-252.

Tarp-Johansen, N. J., & Clausen, N-E.: Design of Wind Turbines in Typhoon area: A first study of Structural Safety of Wind Turbines in Typhoon prone areas. EC-ASEAN Energy Facility, 2006.

Thesbjerg, L. Background for EOG in IEC 61400-1 Edition 3. Unpublished background document, 2007

Thoft-Christensen, P., & Sørensen, J.D. (1982). Reliability of Structural Systems with Correlated Elements. Applied Mathematical Modelling, 6, 171-178.

Toft, H.S.: Probabilistic Design of Wind Turbines. PhD thesis, Aalborg University, 2010.

Veldkamp, D.: Chances in Wind Energy—A Probabilistic Approach to Wind Turbine Fatigue Design. PhD Thesis, DUWIND Delft Univ, Wind Energy Res Institute, Delft, 2006.

Wilkie, D. & C. Galasso: Site-specific ultimate limit state fragility of offshore wind turbines on monopile substructures. Engineering Structures Volume 204, 2020.

Winterstein, S. R., Ude, T. C., Cornell, C. A., Bjerager, P., & Haver, S. (1994). Environmental parameters for extreme response – inverse FORM with omission factors. Structural Safety and Reliability, Vols 1-3, 551–557.